THE
THERMODYNAMIC PROPERTIES
OF
VAPOUR MIXTURES

A thesis presented for the degree of

Doctor of Philosophy in Chemical Engineering

at the

University of Canterbury,

Christchurch, New Zealand

by

T. W. SHANNON

1976

ACKNOWLEDGMENTS

I wish to thank Dr P.J. McElroy for being an understanding and helpful supervisor. The time spent on this project under his supervision has been very worthwhile and, eventually, exciting. Also, thanks are due to Professor A.G. Williamson for his interest in, enthusiasm for, and supervision of (while Dr McElroy was on leave) the project.

This project would not have achieved any success without the skilled assistance of the technical staff (especially Messrs D. Brown, C. Campbell, B. Gordon and N. Foot) of the Chemical Engineering Department for the construction and modification of the apparatus, Mr F. Downing of the Chemistry Department for his glass-blowing, and the vacuum and cryogenic technicians of the Physics Department.

Special thanks are due to: my parents, for their continual encouragement from a distance; Professor A.M. Kennedy, who crystallized my initial wish to carry out a research project and then made sure that I never experienced any financial problems; and latterly to my financee, for her forebearance while I wrote this thesis instead of being pleasant company.

Financial assistance for part of the project was received in the form of Postgraduate Scholarship from Fletcher Industrial Holdings (N.Z.) Ltd and Ivon Watkins-Dow Ltd.

Finally, many thanks are due to Mrs G.D. Niven for her superb layout and typing of this thesis.

CONTENTS

SUMMARY

An apparatus to measure the excess second virial coefficient of gas and/or vapour mixtures has been designed, constructed, developed and tested. Six-litre, stainless steel vessels with all-metal diaphragm valves and an all-metal sensitive capacitance differential pressure transducer were used to construct the apparatus.

The excess second virial coefficient of benzene and cyclohexane vapour mixtures has been determined. The differential nature of the pressure change experiment allows the excess second virial coefficient, ε, and hence the interaction second virial coefficient, B_{12}, to be determined with an accuracy nearly three times better than can be obtained from measurement of the second virial coefficient of the mixture.

ε is determined from a loading pressure, the thermostat temperature and the pressure change on mixing of the two components. Measurements of ε, to between ± 1 and $\pm 10 \times 10^{-6}$ m^3 mol^{-1}, for benzene and cyclohexane, were made at 373, 348, 323, 315 and 298 K. The lower temperature measurements were affected by surface adsorption. A mathematical model has been postulated to calculate a correction for surface adsorption.

A detailed error analysis has been carried out, illustrating the method's robustness, defining the best operating pressures and extreme sensitivity to oil contamination.

CHAPTER 1 INTRODUCTION

1-1 Relevance to Chemical Engineering

Chemical engineers have a great need to be able to understand and predict the P-V-T-x properties of gases, vapours and their mixtures. The most obvious and common application is the ubiquitous distillation operation. Here, a knowledge of the vapour phase chemical potential aids calculation of the liquid-vapour equilibria, so allowing more accurate design of the operational equipment.

Use of general thermodynamic properties with a knowledge of an equation of state has applications to many other chemical engineering unit operations as well, the design of reactors and heat exchangers being two further examples.

On a less applied plane, knowledge of the P-V-T-x properties of gases and vapours has contributed very largely to our understanding of intermolecular forces. The use of this, and future knowledge, with the application of statistical thermodynamic principles, promises to provide the best means of predicting the pure and mixture properties, of both the condensed and gaseous phases.

1-2 Historical Development

Investigations into the P-V-T properties of gases has continued since Robert Boyle's work in 1662. Later workers included Jacques Charles (1802), John Dalton (1801), Amadeo Avagadro (1811) and Amagat (1880).

Their findings can all be summarized in what has come to be known as the perfect gas law, i.e.

$$PV = \sum_i n_i RT \qquad (1\text{-}1)$$

where P is the pressure in Pa

V is the volume in m^3

n_i is the number of moles of component i

R is the universal gas constant = 8.3144 J mol^{-1} K^{-1}

and T is the absolute temperature in K.

The kinetic theory then derived this expression after making an assumption that a gas was made up of non-interacting point particles.

It was only a matter of time before the experimental equipment became sophisticated enough to show that real gases deviated from the simple "perfect gas law". Along with this sophistication, came modified equations of state. These equations were either empirical or had some basis in theory. Amongst the first of these was van der Waal in 1873 with his equation allowing for finite molecule size and molecule interaction. Of the empirical equations, the most successful, initially, was one proposed by Kamerlingh Onnes in 1901. This developed into the so-called "virial equation". Several other equations of state had, and have been, suggested since. These include the Dieterici (in 1899), Berthelot (in 1907) and Redlich-Kwong (in 1949) equations. An even more cumbersome empirical equation of state was proposed, mainly for the high density region, by Benedict, Webb and Rubin in 1940. Other similar equations followed.

1-3 The Virial Equation of State

However, with the development of statistical mechanics and its application to non-ideal gases by Mayer and others, the virial equation was given a theoretical basis. Indeed the virial equation of state may be derived from statistical mechanics (Hill 1962), B being a measure of two-molecule interactions, C the three-molecule interactions, etc.

The virial equation may be expressed in two forms: either the density series, i.e.

$$PV = nRT\left(1 + \left(\frac{n}{V}\right)B(T) + \left(\frac{n}{V}\right)^2 C(T) + \ldots\right) \qquad (1.2)$$

or the pressure series, i.e.

$$PV = nRT + nB'(T)P + nC'(T)P^2 + \ldots \qquad (1.3)$$

where P is the pressure in Pa

V is the volume in m^3

n is the number of moles present

R is the universal gas constant in J mol^{-1} K^{-1}

T is the temperature in K

and B(T), C(T)... are the second and third virial coefficients.

However, for the infinite series, the two sets of coefficients may be related by inverting one series and then comparing coefficients. When done, this gives,

$$B'(T) = B(T) \tag{1.4}$$

and

$$C'(T) = \frac{(C(T) - B^2(T))}{RT} \tag{1.5}$$

It must be stressed though, that this is only for the infinite series.

Experimentally, real behaviour is well described by the virial equation, using the second and third (where known) coefficients at low to moderate pressures (15 bar). At high pressures when the system density approaches liquid proportions, the series diverges.

Statistical thermodynamics gives a direct relationship between the intermolecular potential and B, when there is no angular dependence in the potential, i.e, the molecule is spherically symmetric.

If the intermolecular potential has the form $U(r_{ij})$, then

$$B_{ij}(T) = -2\pi N_A \int_o^\infty (e^{-U(r_{ij})/kT} - 1)r^2 dr \tag{1.6}$$

where i,j refer to the molecule types

K is the Boltzmann constant in $J\,k^{-1}$

r is the distance between the molecules in m

and N_A is the Avagadros number in mol^{-1}.

The relation for the third virial coefficient may be written

$$C_{ij}(T) = -\frac{N_A^2}{3V} \iiint_V (e^{-U(r_{12})/kT} - 1)(e^{-U(r_{13})/kT})(e^{-U(r_{23})/kT} - 1)$$

$$dr_1 dr_2 dr_3 \tag{1.7}$$

For non-spherically symmetric molecules, the relationships become complex as the integrations must now take the relative orientations of the molecules into account. Such relationships are discussed in many references (i.e. Hirschfelder, Curtiss and Bird (1954), Mason and Spurling (1967)). Unfortunately,

measurements of B and C cannot define the intermolecular potential completely, so the search for better empirical potentials, based in theory if possible, goes on.

For a gas or vapour mixture, the second and third virial coefficients of the mixture depend on the composition. Statistical thermodynamics gives a basis to calculate this dependence.

For second virial coefficients,

$$B_m = \sum_{ij}\sum x_i x_j B_{ij} \tag{1.8}$$

which gives, for a binary mixture

$$B_m = x_1^2 B_{11} + 2x_1 x_2 B_{12} + x_2^2 B_{22} \tag{1.9}$$

where B_m is the mixture coefficient in $m^3\ mol^{-1}$

B_{11}, B_{22} are the pure component coefficients in $m^3\ mol^{-1}$

and B_{12} is the second virial coefficient of the unlike molecule interactions also in $m^3\ mol^{-1}$.

Similarly for third virial coefficients, the relations are

$$C_m = \sum_{ijk}\sum\sum x_i x_j x_k C_{ijk} \tag{1.10}$$

and $$C_m = x_1^3 C_{111} + 3x_1^2 x_2 C_{112} + 3x_1 x_2^2 C_{122} + x_2^3 C_{222} \tag{1.11}$$

for the binary mixture.

When talking about binary mixtures, it is convenient to define excess virial coefficients. They may be defined as

$$\varepsilon = B_{12} - \frac{1}{2}(B_{11} + B_{22}) \tag{1.12}$$

$$\mathcal{J}_1 = C_{112} - \frac{1}{3}(2C_{111} + C_{222}) \tag{1.13}$$

and $$\mathcal{J}_2 = C_{122} - \frac{1}{3}(C_{111} + 2C_{222}) \tag{1.14}$$

Using these definitions and equations (1.9) and (1.11) give

$$B_m = x_1 B_{11} + x_2 B_{22} + 2x_1 x_2 \varepsilon \tag{1.15}$$

and

$$C_m = x_1 C_{111} + x_2 C_{222} + 3x_1^2 x_2 \mathcal{J}_1 + 3x_1 x_2^2 \mathcal{J}_2 \tag{1.16}$$

1-4 Corresponding States and Congruence

Having made these definitions and developed these equations, the thermodynamic properties of real gases and vapours may be developed in terms of this particular equation of state. Many references have summarized these properties (e.g. Hirschfelder, Curtiss and Bird, 1954).

Prediction, and initially correlation, of these results requires some unifying theory. How can the B_{12} be related to B_{11} and B_{22}? One possible answer is the use of the principle of corresponding states. This principle gives a method of correlating the behaviour and properties of similar types of molecules, similar in that they all have the same functional form for their intermolecular potential. It uses the critical properties of the compounds as the scaling factor, i.e. for second virial coefficients

$$\frac{B}{V^c} = f(T/T^c) \tag{1.17}$$

The two most common forms of this type of equation are McGlashan and Potter's (1962) equation for n-alkanes, i.e.

$$\frac{B}{V^c} = 0.430 - 0.886\left(\frac{T^c}{T}\right) - 0.694\left(\frac{T^c}{T}\right)^2 - 0.0375(n-1)\left(\frac{T^c}{T}\right)^{4.5} \tag{1.18}$$

where n is the number of carbon atoms in the molecule chain,

and the Pitzer-Curl type correlations, the latest due to Tsonopoulos (1974) where

$$\frac{BP^c}{RT^c} = f(0) + \omega f(1) \tag{1.19}$$

$$\text{for } f(0) = 0.1445 - 0.33\left(\frac{T^c}{T}\right) - 0.1385\left(\frac{T^c}{T}\right)^2 - 0.0121\left(\frac{T^c}{T}\right)^3 - 0.000607\left(\frac{T^c}{T}\right)^8 \tag{1.20}$$

$$f(1) = 0.0637 + 0.331\left(\frac{T^c}{T}\right)^2 - 0.423\left(\frac{T^c}{T}\right)^3 - 0.008\left(\frac{T^c}{T}\right)^8 \tag{1.21}$$

and ω is Pitzer's accentric factor. Tsonopoulos investigated the extension to a very wide range of molecule types. By postulating mixture rules, pseudocritical properties may be predicted to fit the interaction coefficients into the same framework. The most common examples of these are:

for temperature $$T_{12}^c = (T_1^c T_2^c)^{\frac{1}{2}} \quad (1.22)$$

for volume $$V_{12}^c = \frac{1}{8}(V_1^{c\,\frac{1}{3}} + V_2^{c\,\frac{1}{3}})^3 \quad (1.23)$$

for chain length $$n_{12} = \frac{1}{2}(n_1 + n_2) \quad (1.24)$$

and for the accentric factor $$\omega_{12} = \frac{1}{2}(\omega_1 + \omega_2) \quad (1.25)$$

Prausnitz (1969) discusses and modifies these mixing rules to obtain better agreement with experiment.

Another correlating principle utilized to systematize properties of molecules is the Principle of Congruence. Congruence allows the prediction of mixture properties within a family or homologous series from the knowledge of the pure component or other mixture behaviour of that series. For instance, with n-alkanes, if the principle holds, the thermodynamic properties of a mixture only depend on the average chain length of the mixture. Barker and Linton (1963) and Knobler et al (1968) have illustrated the application of the principle of congruence to gas mixture behaviour.

They plotted V^E and H^E/P versus chain length for n-alkanes. They found if they calculated V^E and H^E/P for various compositions of the methane-hexane system they had measured, then other mixtures, with equivalent average chain lengths, also fell on the original methane-hexane system line.

Pandya and Williamson (1971) used Barker and Linton's average chain length concept, McGlashan and Potter's corresponding states treatment for n-alkanes, perfluoro-n-alkanes and n-alk-1-enes, together with expressions for the pure component critical temperature and volume. They combined these three equations to give an expression for the second virial coefficients as a function of n, the chain length, and T only.

1-5 Measurement of Virial Coefficients

It is the purpose of this investigation to design and develop the equipment and techniques required to measure B_{12} with sufficient accuracy to enable the testing of these mixture rules.

It will be shown (see Chapter 3) that

$$\varepsilon \simeq \frac{RT\Delta P}{2x_1 x_2 P^2 (1 + \frac{\Delta P}{P})} \qquad (1.26)$$

where ΔP is the change in system pressure on mixing in Pa

and P is the initial system pressure in Pa.

So then, using equation (1.15), B_{12} may be determined directly and with greater accuracy than other methods (see Chapter 2).

Measurement of ε rather than B_m has other advantages than greater accuracy. ε, itself, is often required in thermodynamic calculations. The system chemical potential of a two-component vapour system may be written in terms of ε, provided that the virial equation truncated at the second term is an adequate description, i.e.

$$\mu_1 = \mu_1^\theta + RT\ln \frac{Py_1}{P^\theta} + P(B_{11} + 2y_2^2 \varepsilon) \qquad (1.27)$$

where μ is the chemical potential in J mol^{-1},

y is the component mole fraction, and

the superscript θ refers to a standard state.

Such equations, as (1.27), may be used to estimate equilibrium yields of gas-phase reactions, for example.

In liquid-vapour equilibria (i.e. multicomponent distillation), it is ε rather than B_m or B_{12} that is required. In a binary system, for instance,

$$RT\ln Py_1 = RT\ln P_1^o x_1 + RT\ln\gamma_1 - (B_{11} - \tilde{V}_1^l)(P - P_1^o) - 2Py_2^2\varepsilon \qquad (1.28)$$

where P^o is the saturation vapour pressure at the temperature T,

x_1 is the mole fraction of component 1 in the liquid phase,

γ is the liquid phase activity coefficient,

and $\tilde{V}^l$ is the liquid phase molar volume in m^3 mol^{-1}.

So for a system of known P^o, γ, $\tilde{V}^l$ and ε, equation (1.28) would allow the calculation of the equilibrium gas phase composition for a given liquid composition. Such an expression may be generalized to a multicomponent system.

Accurate knowledge of interaction coefficients requires, firstly, accurate pure component data. Many methods exist to measure pure component second virial coefficients (Mason and Spurling 1967), the latest of which, due to Couldwell et al (1976), allows for the effect of the third virial coefficient, to give an extrapolation to the zero pressure limit as Scott and Dunlap (1962) pointed out to be necessary.

The temperature function may be determined by a series of determinations of B at various temperatures, but initial trials and calculations suggest that measurement of the isothermal Joule-Thompson coefficient would produce a better defined temperature dependence, i.e.

$$\lim_{P \to 0} \left(\frac{H}{P}\right)_T = B - T\frac{dB}{dT} \qquad (1.29)$$

assuming the effect of the third virial coefficient to be negligible.

The same procedure may be adopted for mixtures of gases, but the errors accumulate rapidly when using equation (1.9) to calculate B_{12} from mixture measurements.

A more accurate procedure, now that precise enough equipment is freely available, is to measure the excess coefficients, i.e. to make a differential measurement, determine ε as defined by equation (1.26) and hence calculate B_{12} using equation (1.15), the errors in ε being far less than those of B_m.

Similarly, instead of measuring the isothermal Joule-Thompson coefficient of the mixture and then using equation (1.9) to back-calculate $T\frac{dB_{12}}{dT}$, it is more accurate to measure the excess heat of mixing of the two components in a flow calorimeter. This can be shown to be related by

$$\Delta_m H^E = 2x_1x_2P\left(\varepsilon - T\frac{d\varepsilon}{dT}\right) \qquad (1.30)$$

Then, once again, equation (1.15) is used to calculate $T\frac{dB_{12}}{dT}$.

So, the four measurements of B_{11}, $\left(\frac{\partial H}{\partial P}\right)_T$, ε and $\Delta_m H^E$, together constitute a set of experiments for the complete determination of the thermodynamic properties of gases, vapours and their mixtures.

As stated earlier, it is the purpose of this investigation to design, build and develop the equipment and techniques to measure the second excess

virial coefficient, ε, for vapours.

CHAPTER 2 A REVIEW OF EXPERIMENTAL METHODS USED TO MEASURE THE INTERACTION SECOND VIRIAL COEFFICIENT

In this chapter, the main techniques used to obtain information on the interaction second virial coefficient are discussed. Using several excellent, recent reviews*, each experimental method is assessed as to its general applicability and likely accuracy.

*Knobler (1976), Couldwell (1975), Cox and Laurenson (1973), Mason and Spurling (1969), McElroy (1968).

2-1 Measurement of the Mixture Second Virial Coefficient

There are many methods that have been used to measure the pure second virial coefficient - Boyle, Burnett, and Gas Density, for example. These methods have been extensively reviewed, explained and their accuracy and limitations discussed (Couldwell (1975), Cox and Laurenson (1973), Mason and Spurling (1969)).

All of these pure component techniques may be used to measure the second virial coefficient of an already mixed gas or vapour, i.e. the mixture is treated as a single gas. The accuracies of the measurements are the same as for the pure component measurements, i.e. $2\text{-}10\times10^{-6}$ m^3 mol^{-1} for gases (i.e. above the critical temperature) and $50\text{-}100\times10^{-6}$ m^3 mol^{-1} for vapours (below the critical temperature) (Dymond and Smith 1968). Invariably the uncertainty in the pressure measurements is a major contributor to the error in B, hence an increase in the pressure measurement precision would reflect in greatly reduced errors in B.

However, the information obtainable on the interaction coefficient will be poor due to the accumulation of experimental errors. If the mixture and pure virial coefficients B are determined to $\pm\delta B$, then, since

$$B_m = x_1^2 B_{11} + 2x_1x_2B_{12} + x_2^2 B_{22} \qquad (1.9)$$

for $x_1 = x_2 = 0.5$,

$$B_{12} = 2B_m - \frac{1}{2}(B_{11} + B_{22}) \qquad (2.1)$$

so that

$$\delta B_{12} = 3\delta B \qquad (2.2)$$

i.e. the error in the interaction coefficient will be three times that of the pure component data. Clearly, unless large effects are being measured, such a set of results would not allow the testing of mixture rules or increase our knowledge of the likely intermolecular behaviour.

2-2 Measurement of the Excess Pressure or Volume on Mixing

The severe error accumulation inherent in the measurement of mixture virial coefficients was recognized and an alternative experiment designed. Edwards and Roseveare (1942), Gorski and Millar (1953), and later McElroy (1968) measured the volume change on mixing of the gases.

Briefly, their method was to load the unmixed gases into separate volumes at equal pressures, measure the pressure, then mix the gases and adjust the volume of the mixing chamber to bring it back to the initial, premixing, pressure as determined by a differential pressure gauge backed to a reference pressure.

If the higher virial coefficients may be ignored, then

$$\varepsilon = \frac{\Delta V}{2x_1 x_2} \tag{2.3}$$

where ΔV is the volume change required to regain the initial loading pressure, and

$$\varepsilon = B_{12} - \frac{1}{2}(B_{11} + B_{22}) \tag{1.12}$$

Hence, as long as the ΔV could be determined to better than half the error in the pure second virial coefficients, the error in the interaction virial coefficient will be the same size as the pure component coefficient. This technique worked well for the permanent gases. McElroy (1968) found that with vapours, and consequential low loading pressures, small ΔV's and a prototype differential pressure transducer he could still obtain results that gave a δB_{12} comparable with the existing δB_{11} and δB_{22}.

With the advent of reliable differential pressure transducers, the equivalent ΔP, constant volume, experiment became a more attractive experiment. In this experiment, the pure components are loaded into separate volumes at equal pressures. The loading pressure is then measured and the gases mixed. Initially a third volume was filled to the loading pressure, isolated and, after mixing, compared with the mixture pressure directly using a differential pressure manometer or transducer.

ε is obtained from the ΔP measured using equation (1.26), viz.

$$\varepsilon \simeq \frac{RT\ P}{2x_1 x_2 P^2} \qquad (1.26)$$

Brewer and Vaughan (1969) had used this technique using an oil manometer for his differential pressure measurement. Obviously this use of the oil manometer is not suitable for organic vapours. However, Brewer's measurements on permanent gas mixtures gave impressively small errors, and he claimed results to $\pm 0.12 \times 10^{-6}$ m^3 mol^{-1} in ε. Knobler et al (1959) had also done similar measurements previously. He claimed an accuracy of 2 to 3×10^{-6} m^3 mol^{-1} or 2 to 3% in ε whichever was the larger.

Measurements of ε for organic vapours was pioneered by Knobler et al (1967, 1968, 1969, 1971). Using a variable reluctance differential pressure transducer capable of measuring a difference of 650 Pa to ±1 Pa, he has been able to measure the excess second virial coefficients of n-alkanes, n-perfluoroalkanes and n-alkane-n-perfluoroalkane mixtures. In all cases he has obtained errors of less than $\pm 40 \times 10^{-6}$ m^3 mol^{-1}, most results being less than $\pm 5 \times 10^{-6}$ m^3 mol^{-1}.

Marsh (1975) has recently presented a method using a Differential Burnett apparatus that allows an extrapolation to zero pressure to evaluate the pure virial coefficients. He claims that the experimental errors are ±1-2, ±7, $\pm 14 \times 10^{-6}$ m^3 mol^{-1} at 40000, 13000 and 6500 Pa.

The vapour under measurement is expanded successively, as is the reference gas (whose second virial coefficient is known accurately, e.g. nitrogen). After each expansion, the difference in pressure between the vapour and the reference is measured. The equality of the successive expansions is ensured by expanding into the same vessel. The vessel is then evacuated before expanding the other gas.

The layout of the apparatus is such that the excess second virial coefficient could be measured using Knobler's technique, but these measurements have not as yet been reported.

Hall and Eubank (1974) have written of a scheme to measure the excess

second virial coefficients and hence the interaction virial coefficients of mixtures using a Burnett apparatus. However, their claimed precision cannot be as high as they claim (0.05% on ΔV^E) as their analysis involves the subtraction of two large, very nearly equal numbers. On reworking their analysis, we get an error of about 130% in ΔV^E. This is not surprising on two accounts as, one, their experiment is basically a measurement of the mixture coefficient, since they do not maintain a reference pressure control, and secondly, their pressure measurement is only good to ±400 Pa. Also, the measurement is to be done at approximately 4 MPa, which is so high that their excess coefficient will not be a measure of two-molecule interactions alone.

2-3 Gas Solubility Methods

The vapour pressure of a component in equilibrium with its condensed phase may be altered by adding an inert gas to the system. Provided the inert gas is only sparingly soluble in the condensed phase, the alteration in the vapour pressure would be caused by two effects: (a) the chemical potential increase of the condensed phase due to the increase in system pressure, and (b) the chemical potential of the vapour phase will be altered due to the interactions between the vapour and inert gas. If the condensed phase is assumed to be incompressible, the observed effects are attributable solely to the vapour-gas interactions.

These effects may be observed by utilizing a static system or a flow system.

Gas chromatography may be used to measure B_{12} also. Here the achieved chromatographic separation, as it varies with total column pressure, is used to evaluate the virial coefficients. The analysis of this technique has been set out by Cruickshank et al (1966). Again it is required that the carrier gas (inert gas) is insoluble in the stationary phase (condensed phase).

Knobler (1976) quotes that under optimal conditions, B_{12} may be determined to $\pm 2 \times 10^{-6}$ m^3 mol^{-1}, but typical uncertainties are

10 to 20×10^{-6} m^3 mol^{-1}. With solubility of the carrier phase in the stationary phase, the uncertainty becomes rapidly larger. This technique, although it promises accurate results, is nonetheless restricted in its applicability.

Once the critical components of the apparatus have been developed, the experiment is relatively straightforward to perform. However, the measurements of other quantities, such as the liquid molar volumes, are required before B_{12} can be calculated. The computation is a rather complex analysis of the data. This, coupled with the very narrow range of systems which may be investigated using this method, means that its application is severely limited.

2-4 Calorimetric Measurements

If two vapours or gases are mixed in an adiabatic flow-calorimeter, then the power required to raise the mixture temperature back to the inlet temperature is a direct measure of ΔH^E on mixing.

As set out in chapter 1 -

$$\frac{\Delta H^E}{2x_1x_2P} = \varepsilon - T\frac{d\varepsilon}{dT} \qquad (1.30)$$

i.e. $$\frac{d\varepsilon}{dT} = \frac{\varepsilon}{T} - \frac{\Delta H^E}{2x_1x_2PT} \qquad (2.4)$$

If ε and $\Delta H^E/P$ are known at one temperature, T_1, say, then integration of $d\varepsilon/dT$ gives

$$\varepsilon(T) = \int_{T_1}^{T} \frac{d\varepsilon}{dT}\,dT + \varepsilon(T_1) \qquad (2.5)$$

Given a set of $\Delta H^E/P$ measurements at various temperatures (T_1 to T_n), equations (2.4 and .5) give a two-level iterative process to evaluate $d\varepsilon/dT$ at each temperature.

Using $\varepsilon(T_1)$, $\frac{\Delta H^E}{P}(T_1)$ and equation (2.4), $(\frac{d\varepsilon}{dT})_{T_1}$ may be evaluated allowing the prediction of $\varepsilon(T_2)$ with some assumed functional form of $\varepsilon = fn(T)$. Hence an estimate of $(\frac{d\varepsilon}{dT})_{T_2}$ can be made. This process is

carried out until there are estimates of the $(\frac{d\varepsilon}{dT})_{T_i}$ at all the n points. These estimates are then curve-fitted with a suitable analytical function and the integration of equation (2.5) performed. The result of this integration is then compared with each of the $\varepsilon(T)$ estimates used in equation (2.4) and the process repeated until the answers give suitable agreement. Unless $(\frac{d\varepsilon}{dT})_T$ is very strongly dependent on $\varepsilon(T)$, this convergence should be straightforward and rapid, using existing numerical techniques.

Since this is a steady-state measurement, adsorption or absorption effects are of very minor consequence (as opposed to the equilibrium measurements of ε at discrete values of T). Careful design (Wormald et al 1969a,b, Mayhew 1976) of the calorimeter will eliminate significant heat leaks. Temperature and power measurements are relatively straightforward, enabling accurate measurements to be made. Wormald (1969a) has used such a calorimeter to measure the isothermal Joule-Thompson coefficient of benzene (the pure component equivalent) to ±10 to ±30x10^{-6} m^3 mol^{-1} in magnitudes ranging from 2 to 4x10^{-3} m^3 mol^{-1}.

However, for mixtures, ±15 to 30% is more usual (Mayhew 1976, Wormald 1969b).

From equation (2.5), the uncertainty in $\varepsilon(T)$ would be

$$\delta\varepsilon(T) = \Delta \int_{T_1}^{T} \frac{d\varepsilon}{dT}\, dT + \delta\varepsilon(T_1) \qquad (2.6)$$

where Δ is the relative error in $d\varepsilon/dT$, assumed constant for simplicity, in this case.

The allowable size of Δ, to make the ΔH^E measurement worthwhile in comparison with the ε measurement may be illustrated by an example.

Rearranging equation (2.6) gives

$$\Delta = \frac{\delta\varepsilon(T_1) + \delta\varepsilon(T)}{\int_{T_1}^{T} \frac{d\varepsilon}{dT}\, dT} \qquad (2.7)$$

Now if ε were determined under optimum conditions (i.e. at 373 K, 66% relative saturation vapour pressure, see Chapter 3), $\delta\varepsilon(T_1)$ could be $\simeq 0.2\text{x}10^{-6}$ m^3 mol^{-1}.

If T_1 = 373 K and T = 323 K with $\varepsilon(T_1) = 20\text{x}10^{-6}$ m^3 mol^{-1} and $\varepsilon(T) = 50\text{x}10^{-6}$ m^3 mol^{-1}, then

$\int_{T_1}^{T} \frac{d\varepsilon}{dT} dT = 30\text{x}10^{-6}$ m^3 mol^{-1} (from equation 2.5), so if $\delta\varepsilon(T) = \pm 8\text{x}10^{-6}$ m^3 mol^{-1} from the ΔP^E measurements, then the equivalent $\Delta\delta\varepsilon$ from the heats of mixing would be

$$\Delta \simeq \pm \frac{8}{30}, \quad \text{i.e.} \quad \pm 25\%$$

Evidently for this case, the H^E route to ε is clearly preferable.

The advantages of this system for obtaining ε vs T is the robustness of the ΔH^E measurement, allowing measurements of ε to be made in regions unattainable with the ΔV^E or ΔP^E measurements, whilst measuring ε at an advantageous temperature. The same number of ΔH^E or $\Delta V^E/\Delta P^E$ measurements would be required to cover the temperature range.

The ΔH^E measurement for mixtures is more accurate than measuring the isothermal Joule-Thompson coefficient of the mixture, as equation (1.9) must be invoked to obtain dB_{12}/dT, causing the errors to escalate rapidly, a situation completely analogous to the mixture second virial coefficient case of section 1.

Together the ΔH^E and ΔP^E measurement techniques promise to give interaction second virial coefficients, over a wide temperature range, to an accuracy determined by the pure component coefficient data alone.

CHAPTER 3 ERROR ANALYSIS AND DESIGN OF THE EXPERIMENT

3-0 Chapter 3 sets out to define the errors that are likely to be incurred whilst using a differential method of measuring the excess second virial coefficient.

These errors can be broadly classified into two categories:

(i) errors inherent in the physical measurements, e.g. temperature, pressure, and change in pressure; and

(ii) errors caused by the unmeasurable extensive properties of the system, e.g. the number of moles in the vapour phase.

This analysis will attempt to define the technique's sensitivity and range of applicability.

Throughout this chapter, we will derive expressions for the corrections required to allow the measured quantities to be related to the "real" or "true" values of ε that we require. So, we will use $\varepsilon_{apparent}$ to mean the value of ε that arises when one assumes no corrections. Then the correction $\delta\varepsilon$ required to obtain the "true" ε is simply

$$\delta\varepsilon = \varepsilon - \varepsilon_{apparent}$$

However, this definition brings with it, a second effect; namely, the idea of "true" and "apparent" mole fractions.

In Appendix I it is shown that, in our situation, the effect caused by neglecting the correction to the apparent mole fraction is insignificant compared with the effect caused by the altered measured variable.

3-1 Basic Relationships

Referring to figure 3-1, if we fill two equal-sized volumes to equal pressures with differing components, we can write, using the pressure series Virial Equation of State:

$$PV = n_1(RT + B'_{11}P + C'_{111}P^2 + \ldots) \tag{3.1}$$

for volume 1, and

$$PV = n_2(RT + B'_{22}P + C'_{222}P^2 + \ldots) \tag{3.2}$$

for volume 2

where P is the pressure within the volumes (Pa)

V is the volume (m^3)

T is the temperature of the vapour (K)

R is the universal gas constant = 8.3144 J mol^{-1} K^{-1}

n_i is the number of moles of gas within the volume i

B'_{ij} is the second virial coefficient of the pressure series (m^3 mol^{-1}).

In the infinite series

B' = B, where B is the volume series second virial coefficient,

C' is the third pressure series virial coefficient (m^3 mol^{-1} Pa^{-1}),

C' = $(C - B^2)/RT$ in the infinite series, where C is the volume series third virial coefficient((m^3 mol^{-1})^2)

The subscripts indicate the component.

Upon mixing and allowing the temperature to return to the original value again, we may write

$$P_m(2V) = (n_1 + n_2)(RT + B_mP_m + C'_mP_m^2 + \ldots) \tag{3.3}$$

where the subscript m stands for the mixture.

Rewriting equations (3.1,3.2,3.3) in terms of V, then adding (3.1 and 3.2) and finally dividing the resulting two equations by $(n_1 + n_2)$ gives

$$\frac{2V}{n_1+n_2} = \frac{RT}{P} + x_1B_{11} + x_2B_{22} + (x_1C'_{111} + x_2C'_{222})P + \ldots \tag{3.4}$$

$$= \frac{RT}{P_m} + B_m + C'_mP_m + \ldots \tag{3.5}$$

$$\text{i.e. } B_m - x_1B_{11} - x_2B_{22} = RT\left(\frac{1}{P} - \frac{1}{P_m}\right) - C'_mP_m + (x_1C'_{111} + x_2C'_{222})P \tag{3.6}$$

where x_i is the mole fraction of component i, i.e. $x_i = \frac{n_i}{\sum_i n_i}$.

From statistical thermodynamics

$$B_m = x_1^2 B_{11} + x_2^2 B_{22} + 2x_1x_2B_{12} \qquad (1.9)$$

and so, using the definition for the excess second virial coefficient given in Chapter 1, i.e.

$$\varepsilon = B_{12} - \frac{1}{2}(B_{11} + B_{22}) \qquad (1.12)$$

then

$$B_m = x_1B_{11} + x_2B_{22} + 2x_1x_2\varepsilon \qquad (1.15)$$

Similarly, for the third virial coefficients

$$C'_m = x_1^3 C'_{111} + x_2^3 C'_{222} + 3x_1^2 x_2 C'_{112} + 3x_1x_2^2 C'_{122} \qquad (1.11)$$

and the two excess coefficients defined in Chapter 1, i.e.

$$\mathfrak{Z}'_1 = C'_{112} - \frac{1}{3}(2C'_{111} + C'_{222}) \qquad (1.13)$$

and

$$\mathfrak{Z}'_2 = C'_{122} - \frac{1}{3}(C'_{111} + 2C'_{222}) \qquad (1.14)$$

then*

$$C'_m = x_1C'_{111} + x_2C'_{222} + 3x_1x_2(x_1\mathfrak{Z}'_1 + x_2\mathfrak{Z}'_2) \qquad (1.16)$$

Finally, defining $P_m = P + \Delta P$ (3.7)

and then substituting (1.15, .16 and 3.7) into equation (3.6) gives

$$2x_1x_2\varepsilon = \frac{RT\Delta P}{P^2(1+\frac{\Delta P}{P})} - 3x_1x_2(x_1\mathfrak{Z}'_1 + x_2\mathfrak{Z}'_2)P - (3x_1x_2(x_1\mathfrak{Z}'_1 + x_2\mathfrak{Z}'_2) + x_1C'_{111} + x_2C'_{222})\,\Delta P \qquad (3.8)$$

The mole fractions, x_1 and x_2, may be evaluated by using equations (3.1 and 3.2) to calculate (n_1/V) and (n_2/V) (assuming the volumes to be equal - see section 2). These may be substituted into equation (3.8) or evaluated separately. We choose to evaluate separately for clarity.

This analysis has two advantages over that developed by Knobler (1968) (see Appendix II). Firstly, it is not iterative, and secondly it indicates, directly, how the third virial coefficients will affect the extrapolation to

*NOTE: Since B = B' in the infinite series, $\varepsilon = \varepsilon'$, but $\mathfrak{Z}'$ is a complex function of $\mathfrak{Z}$, B and ε.

zero pressure, i.e. a plot of $\varepsilon_{apparent}$ vs P

where $\varepsilon_{apparent} = \dfrac{RT\Delta P}{2x_1x_2P^2(1+\frac{\Delta P}{P})}$ would be very nearly linear.

However, Knobler's analysis has the advantage that the final expression uses the volume series virial coefficients directly.

3-2 Measurement Errors

It will be shown in the next section that the first term on the right-hand side of equation 3.8 is the dominant term, i.e. we will use

$$\varepsilon = \frac{RT\Delta P}{2x_1x_2P^2(1+\frac{\Delta P}{P})} \tag{3.9}$$

for the error analysis.

The measured variables are ΔP, P and T. The calculation of x_1 and x_2 depend on P and T and the assumption of equal mixing volumes. The following analysis attempts to relate these parameters.

Using the usual δ-notation for errors, we get from equation (3.9)

$$\frac{\delta\varepsilon}{\varepsilon} = \frac{\delta T}{T} + \frac{\delta\Delta P}{\Delta P} + 2\frac{\delta x}{x} + \frac{2P\delta P + P\delta\Delta P + \Delta P\delta P}{P^2 + P\Delta P}$$

$$= \frac{\delta T}{T} + \frac{\delta\Delta P}{\Delta P} + 2\frac{\delta x}{x} + \frac{2\delta P}{P+\Delta P} + \frac{\delta\Delta P}{P+\Delta P} + \frac{\Delta P\delta P}{P^2+P\Delta P}$$

Since both ΔP and $\delta\Delta P$ $<<$P, this simplifies to

$$\frac{\delta\varepsilon}{\varepsilon} = \frac{\delta T}{T} + \frac{\delta\Delta P}{\Delta P} + 2\frac{\delta x}{x} + 2\frac{\delta P}{P} \tag{3.10}$$

The $\frac{\delta x}{x}$ term in equation (3.10) is further dependent on P, T and the equality of mixing volumes.

The inequality of the mixing volumes is a second-order effect (see Appendix III) and so will be ignored.

Now, we may write

$$(x_1 + \delta x_1) = \frac{n_1 + \delta n}{n_1+n_2+2\delta n} \tag{3.11}$$

if we assume that $\delta n_1 = \delta n_2 = \delta n$. Upon multiplying out and recollecting the terms, this transforms to

$$\frac{\delta x_1}{x_1} = \frac{\delta n}{n_i} + \frac{2\delta n}{(n_1+n_2)} \qquad (3.12)$$

since we require the maximum error.

In our experiment $n_1 \simeq n_2$, so equation (3.12) now approximates to

$$\frac{\delta x}{x} = \frac{2\delta n}{n} \qquad (3.13)$$

Now using the perfect gas law, we get

$$\frac{(\delta n/V)}{(n/V)} = \frac{\delta T}{T} + \frac{\delta P}{P} \qquad (3.14)$$

giving

$$\frac{\delta x}{x} = 2\left(\frac{\delta T}{T} + \frac{\delta P}{P}\right) \qquad (3.15)$$

Substituting this result into equation (3.10), we get, finally,

$$\frac{\delta \varepsilon}{\varepsilon} = \frac{\delta \Delta P}{\Delta P} + 5\,\frac{\delta T}{T} + 5\,\frac{\delta P}{P} \qquad (3.16)$$

The relative sizes of each term can be illustrated by taking a hypothetical situation. The pressure difference can be read (including the zero-error) to ±0.1 Pa, the thermostat temperatures can be held to ±0.02 K, whilst the absolute pressure may be determined to ±10 Pa. Taking a case where $T = 320$ K, $P = 20000$ Pa, $\Delta P = 5$ Pa, gives a value of $\varepsilon = 66.5\times10^{-6}$ m^3 mol^{-1} (using equation 3.9 with $x_1 = x_2 = 0.5$).

Substituting these values into equation (3.16)

$$\delta\varepsilon = \pm 66.5\times10^{-6}\left(\frac{0.1}{5} + \frac{5\times0.02}{320} + \frac{5\times10}{20000}\right)$$

$$= \pm 66.5\times10^{-6}\,(0.02 + 0.0003 + 0.0025)$$

i.e. $\varepsilon = (66.5\pm1.4)\times10^{-6}$ m^3 mol^{-1};

showing that the major source of error is in the measurement of the pressure difference. This effect would be even more pronounced at lower loading pressures as halving the loading pressure reduces the pressure difference fourfold for a given ε value. Hence the relative error in the pressure difference increases fourfold whilst the relative pressure error only doubles.

3-3 The Effect of the Third Virial Coefficients

The third virial coefficients cause the extrapolation of the excess second virial coefficient to the zero pressure limit to have a non-zero slope. The effect is defined by equation (3.8), i.e.

$$\varepsilon = \frac{RT\Delta P}{2x_1x_2P^2(1+\frac{\Delta P}{P})} - \frac{3}{2}P(1+\frac{\Delta P}{P})(x_1\mathcal{J}_1' + x_2\mathcal{J}_2') - \frac{\Delta P}{2x_1x_2}(x_1C'_{111} + x_2C'_{222}) \quad (3.8)$$

where

$$\mathcal{J}_1' = C'_{112} - \frac{1}{3}(2C'_{111} + C'_{222}) \quad (1.13)$$

$$\mathcal{J}_2' = C'_{122} - \frac{1}{3}(C'_{111} + 2C'_{222}) \quad (1.14)$$

and $$C' = \frac{(C - B^2)}{RT} \quad (1.5)$$

Rearranging equation (3.8) since

$$\frac{RT\Delta P}{2x_1x_2P^2(1+\frac{\Delta P}{P})} = \varepsilon_{apparent}$$

gives

$$\delta\varepsilon = -\frac{3}{2}P(1+\frac{\Delta P}{P})(x_1\mathcal{J}_1' + x_2\mathcal{J}_2') - \frac{\Delta P}{2x_1x_2}(x_1C'_{111} + x_2C'_{222}) \quad (3.17)$$

Cheuh and Prausnitz (1967) have presented a corresponding states type correlation for estimating the third virial coefficient of non-polar gases. Whilst the calculation we require falls outside their range of applicability, it will give us a sufficiently good estimate of the third virial coefficient for our purposes.

Using the critical constants of T^c = 562.1 K, V^c = 2.6×10^{-4} m^3 mol^{-1} for benzene, and T^c = 553.2 K and V^c = 3.08×10^{-4} m^3 mol^{-1} for cyclohexane, gives at 320 K $T_{r\ benzene}$ = 0.57 and $T_{r\ cyclohexane}$ = 0.58.

From the Cheuh and Prausnitz plot, this gives

$$(C/V^{c2})_{benzene} = -3.8, \quad \text{i.e. } C_{benzene} = -2.6\times10^{-7}\ (m^3\ mol^{-1})^2$$

and

$$(C/V^{c2})_{cyclohexane} = -3.8, \quad \text{i.e. } C_{cyclohexane} = -3.6\times10^{-7}\ (m^3\ mol^{-1})^2$$

Using equations (1.13,1.14 and 1.5) gives

$$C'_{111} = -6.7\text{x}10^{-10}\ m^3\ mol^{-1}\ Pa^{-1}$$

$$C'_{222} = -7.5\text{x}10^{-10}\ m^3\ mol^{-1}\ Pa^{-1}$$

$$\mathcal{F}'_1 = 6.7\text{x}10^{-12}\ m^3\ mol^{-1}\ Pa^{-1}$$

and $$\mathcal{F}'_2 = -2.7\text{x}10^{-11}\ m^3\ mol^{-1}\ Pa^{-1}$$

C'_{112} and C'_{122} were calculated using the approximation suggested by Orentlicher (Mason and Spurling, 1967, p 260), i.e.

$$C_{ijk} \simeq (C_{iii}C_{jjj}C_{kkk})^{1/3} \qquad (3.18)$$

Evaluating equation (3.8) using the data in section 3-2 and the third virial coefficients gives

$$\delta\varepsilon = 1.5\text{x}10^{-11}\ P + 7.1\text{x}10^{-9}\ m^3\ mol^{-1}$$

The $1.5\text{x}10^{-11}$ coefficient on the P term is very insensitive to the absolute values of the third virial coefficient due to equations (1.13 and .14). In fact, if $(C/V^{C^2}) = 0.5$ the slope of the extrapolation changes sign and has a value of $7.5\text{x}10^{-12}\ m^3\ mol^{-1}\ Pa^{-1}$, i.e. extrapolation from 100 kPa to 0 Pa involves a correction of $-7.5\text{x}10^{-7}\ m^3\ mol^{-1}$ instead of a correction of $1.5\text{x}10^{-6}\ m^3\ mol^{-1}$.

So an extrapolation neglecting the effect of the third virial coefficients could cause a systematic error of about $\pm 2\text{x}10^{-6}\ m^3\ mol^{-1}$ for a 10^5 Pa pressure range. Since our experiments are likely to be carried out at about 2 to $3\text{x}10^4$ Pa, the error due to disregarding the third virial coefficients is likely to be about $\pm 0.5\text{x}10^{-6}\ m^3\ mol^{-1}$.

3-4 The Effect of Impure and Inert Vapours

The effect of inert gases or impure vapours in the mixture may be gauged by treating the system as a multicomponent mixture. So, by extending the mixture definitions, the size of the allowable impurity can be calculated.

Going back to section 3-1 and figure 3-1, we may rewrite equation (3.1) in terms of a third component, n_6, i.e.

$$PV = (n_1 + n_6)RT + (n_1 + n_6)B_{m6}P + \ldots \quad (3.19)$$

where B_{m6} is the second virial coefficient of the binary mixture of component (1) and impurity (6).

As before, equation (3.2) is

$$PV = n_2RT + n_2B_{22}P + \ldots \quad (3.2)$$

truncating the series at the second term.

Equation (3.3), describing the mixture, now becomes

$$2P_mV = (P+\Delta P)(2V) = (n_1+n_2+n_6)RT + (n_1+n_2+n_6)B_m(P+\Delta P) \quad (3.20)$$

$$\text{i.e. } 2V = \frac{(n_1+n_2+n_6)RT}{(P+\Delta P)} + \frac{n_1(n_1+n_2)}{n_1+n_2+n_6}B_{11} + \frac{n_2(n_1+n_2)}{n_1+n_2+n_6}B_{22} + \frac{2n_1n_2\varepsilon}{n_1+n_2+n_6}$$

$$+ \frac{n_6^2}{n_1+n_2+n_6}B_{66} + \frac{2n_1n_6}{n_1+n_2+n_6}B_{16} + \frac{2n_2n_6}{n_1+n_2+n_6}B_{26}, \ldots \quad (3.21)$$

after using equation (1.12), i.e.

$$\varepsilon = B_{12} - \frac{1}{2}(B_{11} + B_{22})$$

the definition (1.8) for the mixture

$$B_m = x_1^2B_{11} + x_2^2B_{22} + x_6^2B_{66} + 2x_1x_2B_{12} + 2x_1x_6B_{16} + 2x_2x_6B_{26}$$

Adding equations (3.19) and (3.2), and writing (again using definition (1.8))

$$B_{m6} = x_1^2B_{11} + 2x_1x_6B_{16} + x_6^2B_{66} \quad \text{and rearranging gives}$$

$$2V = (n_1+n_2+n_6)\frac{RT}{P} + \frac{n_1^2}{n_1+n_6}B_{11} + \frac{2n_1n_6}{n_1+n_6}B_{16} + \frac{n_6^2}{n_1+n_6}B_{66} + n_2B_{22} \quad (3.22)$$

Equating equations (3.21) and (3.22) now gives

$$(n_1+n_2+n_6)\frac{RT}{P}\left(1 - \frac{1}{1+\frac{\Delta P}{P}}\right) = \frac{2n_1n_2\varepsilon}{n_1+n_2+n_6} + \left(\frac{n_1(n_1+n_2)}{n_1+n_2+n_6} - \frac{n_1^2}{n_1+n_6}\right)B_{11}$$

$$+ \left(\frac{n_2(n_1+n_2)}{n_1+n_2+n_6} - n_2\right)B_{22} + \left(\frac{2n_1n_6}{n_1+n_2+n_6} - \frac{2n_1n_6}{n_1+n_6}\right)B_{16}$$

$$+ \frac{2n_1n_6}{n_1+n_2+n_6}B_{26} + \left(\frac{n_6^2}{n_1+n_2+n_6} - \frac{n_6^2}{n_1+n_6}\right)B_{66} \quad (3.23)$$

Multiplying both sides of equation (3.23) by $\frac{n_1+n_6}{(n_1+n_2+n_6)(n_1+n_6)}$

and simplifying, gives

$$\delta\varepsilon = -\frac{x_6}{2(x_1+x_6)} B_{11} + \frac{x_6}{2x_1} B_{22} + \frac{x_6}{(x_1+x_6)} B_{16} - \frac{x_6}{x_1} B_{26} + \frac{x_6^2}{2x_1(x_1+x_6)} B_{66} \qquad (3.24)$$

since $\varepsilon_{apparent} = \frac{RT\Delta P}{2x_1x_2P^2(1+\frac{\Delta P}{P})}$

The impurity present, was likely to have arisen from either, or both, of two sources: residual mixture in the mixing volumes from the previous run, or inert gases left from the degassing procedure.

Firstly, the amount of residual mixture left can be calculated using the perfect gas law. The volume of one cylinder was 6×10^{-3} m^3 and each cylinder may be evacuated to at least 0.1 Pa. At 300 K, this represents 2×10^{-7} moles. A typical vapour loading would be 5×10^{-2} moles, so the residual would give a mole fraction of about 5×10^{-6}.

During the sample degassing, the degassing chamber was continuously evacuated to remove any inerts before the vapour sublimation occurs. The degasser has a volume of about 10^{-3} m^3 and was run at a pressure of about 10 Pa. Each degassing run handled about 0.5 moles of fluid. Again using the perfect gas law, the maximum number of moles of impurity that may be present (assuming that the vapour space was completely impurity and at a temperature of 300 K) would be 4×10^{-6} moles, giving an impurity mole fraction of 10^{-5} to the degassed batch.

So, using $x_1 = 0.49$, $x_2 = 0.5$, $x_3 = 0.01$, as an extreme case, and assuming that the impurity is nitrogen or carbon dioxide, i.e. $B_{66} \simeq -10^{-5}$ m^3 mol^{-1}, then with $B_{11} = -1.2\times10^{-3}$ m^3 mol^{-1}, $B_{22} = -1.3\times10^{-3}$ m^3 mol^{-1} and using the arithmetic mean to calculate the interaction coefficients, equation (3.24) gives

$$\delta\varepsilon = \pm2.0\times10^{-9} \text{ m}^3 \text{ mol}^{-1}$$

This is probably a maximum error as the degassed vapour space was unlikely to be all inert gas, levels of 0.01 to 0.1 Pa are much more likely, and secondly, any organic vapour impurity was likely to have a second virial coefficient of the order of -10^{-3} m^3 mol^{-1}.

3-5 The Effect of Unequal Loading Pressures

Referring to figure 3.1, we may write the equations of state for each volume as before (in section 1) (i.e. equal volumes, equal temperatures)

$$PV = n_1(RT + B_{11}P + \ldots) \tag{3.1}$$

However, assuming that the loading pressure in the second volume is $(P+\delta P)$ causes equation (3.2) to be rewritten as

$$(P+\delta P)V = n_2(RT + B_{22}(P+\delta P) + \ldots) \tag{3.28}$$

where δP is some small pressure error.

Upon mixing, we get, as before (see section 1)

$$P_m(2V) = (n_1+n_2)(RT + B_m P_m + \ldots) \tag{3.3}$$

Rewriting these equations in terms of V, dividing by (n_1+n_2) and using $P_m = P+\Delta P$ gives

$$\frac{V}{(n_1+n_2)} = \frac{x_1 RT}{P} + x_1 B_{11} \tag{3.29}$$

$$= \frac{x_2 RT}{P+\delta P} + x_2 B_{22} \tag{3.30}$$

and

$$\frac{2V}{n_1+n_2} = \frac{RT}{P+\Delta P} + B_m \tag{3.31}$$

Subtracting (3.29) and (3.30) from (3.31) and substituting for B_m using equation (1.15), i.e.

$$2x_1x_2\varepsilon = B_m - x_1B_{11} - x_2B_{22} \quad \text{gives}$$

$$2x_1x_2\varepsilon = \frac{x_1RT}{P} + \frac{x_2RT}{(P+\delta P)} - \frac{RT}{P+\Delta P} \tag{3.32}$$

$$= \frac{x_1RT}{P} + \frac{x_2RT}{P(1+\frac{\delta P}{P})} - \frac{RT}{P(1+\frac{\Delta P}{P})}$$

using the binomial expansionto the linear term on the $(1 + \frac{\delta P}{P})^{-1}$ factor gives

$$= \frac{RT}{P}\left(1 - \frac{1}{(1+\frac{\Delta P}{P})}\right) - \frac{x_2 RT\delta P}{P^2}$$

$$= \frac{RT\Delta P}{P^2(1+\frac{\Delta P}{P})} - \frac{x_2 RT\delta P}{P^2}$$

Since $\frac{RT\Delta P}{P^2(1+\frac{\Delta P}{P})} = 2x_1x_2\,\varepsilon_{apparent}$, this final form becomes

$$\delta\varepsilon = \pm\frac{RT\delta P}{2x_1P^2} \qquad (3.33)$$

If the loading pressures can be balanced to 0.1 Pa, i.e. $\delta P = \pm 0.1$ Pa, then using the particular example used in section 2, gives on substitution into equation (3.33)

$$\delta\varepsilon = \pm 0.7\times10^{-6}\ m^3\ mol^{-1}$$

Since δP will probably be two to ten times less than the δP used, this error is not likely to be significant when compared with the other uncertainties.

3-6 The Effect of Changing the Total Number of Moles in the Vapour Phase during the Experiment

The basic assumption inherent in the analysis developed up to this point has been that the total number of moles in the vapour phase remain constant. This section will look at the consequences of this assumption not holding and the sensitivity of the experiment to it.

The number of moles in the vapour phase may be altered by three possible mechanisms in our case. These are:

(i) Solution into residual traces of oil in the cylinders;

(ii) Adsorption to the vessel walls; and

(iii) Capillary condensation.

3-6.1 Vapour Solution in Oil

If there is a trace of oil in one of the cylinders, some solution of each component will occur, depending primarily on the partial saturation vapour pressure of that component. The amount of vapour going into solution will alter throughout the experiment if the oil is in one of the mixing cylinders. If the oil is in the reference cylinder, the results will have a positive bias.

The analysis has two parts: one, the effect of oil in one of the mixing cylinders, and two, the effect of oil in the reference cylinder.

Firstly, the effect of oil in one of the mixing cylinders:-

Referring to figure 3.2, if we assume that

$V_1 = V_2 = V_{ref} = V$ and initially

$P_1 = P_2 = P_{ref} = P$; then for volumes 1 and 2

$$PV = n_1RT + n_1B_{11}P + \ldots \tag{3.34}$$

$$PV = (n_2-n_2')RT + (n_2-n_2')B_{22}P + \ldots \tag{3.35}$$

where $$n_2' = \frac{P}{P_2^o} N_2 , \tag{3.36}$$

using Raoult's law,

n_2' is the number of moles of component 2 in oil solution,

N_2 is the number of moles of oil present (in cylinder 2, say)

and P_2^o is the saturation vapour pressure of component 2 at temperature T.

After mixing

$$(P+\Delta P)(2V) = (n_1+n_2-n_1''-n_2'')RT + (n_1+n_2-n_1''-n_2'')B_m(P+\Delta P) + \ldots \tag{3.37}$$

where $$n_1'' = \frac{PN_2}{2P_1^o} \tag{3.38}$$

and

$$n_2'' = \frac{PN_2}{2P_2^o} \tag{3.39}$$

applying Raoult's law again, this time, to the mixture.

Rearranging equations (3.34, .35 and .37) and using $P_m = P+\Delta P$, gives

$$B_{11} = \frac{V}{n_1} - \frac{RT}{P} \tag{3.40}$$

$$B_{22} = \frac{V}{(n_2-n_2')} - \frac{RT}{P} \tag{3.41}$$

$$B_m = \frac{2V}{(n_1+n_2-n_1''-n_2'')} - \frac{RT}{P+\Delta P} \tag{3.42}$$

Since $2x_1x_2\varepsilon = B_m - x_1B_{11} - x_2B_{22}$ (1.15)

then using equations (3.40 to .42)

$$2x_1x_2\varepsilon = \frac{2V}{(n_1+n_2-n_1''-n_2'')} - \frac{RT}{(P+\Delta P)} + \frac{x_1RT}{P} + \frac{x_2RT}{P} - \frac{V}{n_1+n_2} - \frac{n_2V}{(n_2-n_2')(n_1+n_2)}$$

$$= \frac{RT}{P}\left(1 - \frac{1}{P+\Delta P}\right) + V\left\{\frac{2}{(n_1+n_2-n_1''-n_2'')} - \frac{1}{(n_1+n_2)} - \frac{n_2}{(n_2-n_2')(n_1+n_2)}\right\}$$

$$= \frac{RT\Delta P}{P^2\left(1+\frac{\Delta P}{P}\right)} + \frac{V}{(n_1+n_2)}\left\{\frac{2}{1-\left(\frac{n_1''+n_2''}{n_1+n_2}\right)} - 1 - \frac{n_2}{(n_2-n_2')}\right\}$$

$$= 2x_1x_2\,\varepsilon_{apparent} + \frac{V}{n_1+n_2}\left\{\frac{1+\left(\frac{n_1''+n_2''}{n_1+n_2}\right)}{1-\left(\frac{n_1''+n_2''}{n_1+n_2}\right)} - \frac{1}{\left(1-\frac{n_2'}{n_2}\right)}\right\} \tag{3.43}$$

Applying the binomial expansion to the $\left(1 - \frac{n_1''+n_2''}{n_1+n_2}\right)$ and $\left(1 - \frac{n_2'}{n_2}\right)$ terms and ignoring all second and higher order terms gives

$$2x_1x_2\delta\varepsilon = \frac{V}{n_1+n_2}\left\{1 + \frac{2(n_1''+n_2'')}{n_1+n_2} - \left(1+\frac{n_2'}{n_2}\right)\right\}$$

$$\text{i.e.}\quad \delta\varepsilon = \frac{P.V.N.}{2n_1n_2}\left\{\frac{1}{P_1^o} + \frac{1}{P_2^o} - \frac{(n_1+n_2)}{n_2P_2^o}\right\} \tag{3.44}$$

upon substituting for n_1'', n_2'' and n_2' using equations (3.38, .39 and .36).

If the subscripts in equation (3.44) were interchanged, the sign of $\delta\varepsilon$ changes. This is equivalent to loading the other component into the volume containing the oil first. So, the effect would manifest itself by causing

a difference in the observed results of $2\delta\varepsilon$, each result depending upon which component was loaded into the contaminated cylinder first.

The second part of the analysis concerns having a trace of oil in the reference volume.

Again referring to figure 3.2, using the same notation as previously and assuming that all the volumes are equal (for clarity), we get:

$$P_1V = n_1RT + n_1B_{11}P_1 \tag{3.45}$$

for the first volume.

On measuring the loading pressure in the reference volume and the subsequent balancing of the pressure in volume 2 gives

$$PV = (n_1 - n_1')RT + (n_1 - n_1')B_{11}P \tag{3.46}$$

for the loading pressure, and

$$PV = n_2RT + n_2B_{22}P \tag{3.2}$$

for volume 2, where

$$n_1' = N\frac{P}{P_1^o} \quad \text{by Raoult's law} \tag{3.47}$$

and N is the number of moles of oil in the reference volume.

On mixing:

$$P_m(2V) = (n_1 + n_2)RT + (n_1 + n_2)B_mP_m \tag{3.3}$$

If we define, as usual

$$P_m = P + \Delta P \tag{3.7}$$

and also

$$P_1 = P + \delta P \tag{3.48}$$

then rewriting equations (3.2, .45 and .46) gives

$$\frac{V}{(n_1+n_2)} = \frac{x_1RT}{P-\delta P} + x_1B_{11}$$

$$\frac{V}{(n_1+n_2)} = \frac{x_2RT}{P} + x_2B_{22}$$

and

$$\frac{2V}{(n_1+n_2)} = \frac{RT}{P+\Delta P} + B_m$$

Combining these three equations in the usual way, gives

$$2x_1x_2\varepsilon = 2x_1x_2\,\varepsilon_{apparent} + \frac{RT\delta P}{P^2} \qquad (3.49)$$

Subtracting (3.46) from equation (3.45) gives

$$(P_1-P)V = \delta PV = n_1'RT + n_1B_{11}\delta P + n_1'B_{11}P$$

i.e. $$\delta P \simeq \frac{n_1'}{V}(RT+B_{11}P)\left(1 + \frac{n_1B_{11}}{V}\right) \qquad (3.50)$$

using the binomial expansion to the linear term on the $\left(1 - \frac{n_1B_{11}}{V}\right)^{-1}$ factor.

Substituting this result into equation (3.49) and using equation (3.47) and assuming that the $(B_{11}P)/V$ and $(n_1B_{11})/V^2$ terms are negligible compared with the RT/V term, we get

$$\delta\varepsilon = \frac{N(RT)^2}{2x_2PP_1^{o}V} \qquad (3.51)$$

The effect of a minute amount of oil in either one of the mixing or the reference volumes or both, is illustrated in figure 3.3.

The effects so illustrated were calculated using:

(i) the amounts of oil given in the figure key (note the use of the binomial theorem was valid);

(ii) component 1 as benzene, component 2 as cyclohexane;

(iii) the saturation vapour pressures were evaluated using a modified Antione equation with parameters from the Handbook of Chemistry and Physics (Weast 1970);

(iv) the second virial coefficients were evaluated using the McGlashan-Potter equation (McGlashan and Potter 1962) with the Wormald-Guggenheim values for the chain-length parameters: 4.0 and 3.5 for benzene and cyclohexane;

(v) finally the loading pressure was arbitrarily chosen to be 60% of the saturation vapour pressure at the given temperature.

3-6.2 Surface Adsorption

A second mechanism for altering the total number of moles in the vapour phase could be surface adsorption. The effect of mixing is to halve the partial pressure and double the surface area. Unless the adsorption isotherm is such that halving the partial pressure halves the adsorption, a change in the total pressure will result.

Referring to figure 3.2 once more, we may write

$$PV = (n_1-n_1')RT + (n_1-n_1')B_{11}P + \ldots \quad (3.52)$$

$$= (n_2-n_2')RT + (n_2-n_2')B_{22}P + \ldots \quad (3.53)$$

for the cylinders Mix 1 and 2 on loading, where n_1' and n_2' refer to the number of moles adsorbed on to the surface of each cylinder before mixing.

After the mixing

$$(P+\Delta P).2V = (n_1+n_2 - n_1'' - n_2'')RT + (n_1+n_2-n_1''-n_2'')B_m(P+\Delta P) \quad (3.54)$$

where n" refers to the moles adsorbed after mixing.

Rearranging equations (3.52, .53 and .54) gives

$$B_m = \frac{2V}{(n_1+n_2-n_1''-n_2'')} - \frac{RT}{(P+\Delta P)}$$

$$x_1B_{11} = \frac{n_1V}{(n_1+n_2)(n_1-n_1')} - \frac{x_1RT}{P}$$

and

$$x_2B_{22} = \frac{n_2V}{(n_1+n_2)(n_2-n_2')} - \frac{x_2RT}{P}$$

Combining these equations then gives

$$2x_1x_2\varepsilon = 2x_1x_2\,\varepsilon_{apparent} + \frac{V}{(n_1+n_2-n_1''-n_2'')}\left\{2 - \frac{(n_1-n_1'')}{(n_1-n_1')} - \frac{(n_2-n_2'')}{(n_2-n_2')}\right\}$$

$$\text{i.e. } \delta\varepsilon \simeq \frac{(n_1+n_2)}{2n_1n_2}V\left\{\frac{n_1''-n_1'}{n_1} + \frac{n_2''-n_2'}{n_2}\right\} \quad (3.55)$$

To evaluate the effect of surface adsorption, a standard B.E.T. isotherm was used, together with the assumption that the mixture isotherm was a linear combination of the individual isotherms.

The B.E.T. isotherm can be written as

$$n' = \frac{N^{o} Ac \frac{P}{P^{o}}}{(1 - \frac{P}{P^{o}})(1 + (C-1)\frac{P}{P^{o}})} \qquad (3.56)$$

where N^{o} is the number of moles per unit area required to form a monolayer (in mol m^{-2})

C is an isotherm parameter, usually about 100 for the adsorption of a nonpolar substance on to a polar substrate,

and A is the adsorptive area.

Consequently

$$n'' = \frac{N^{o} Ac \frac{P}{P^{o}}}{(1 - \frac{P}{2P^{o}})(1 + (C-1)\frac{P}{2P^{o}})} \qquad (3.57)$$

if the cylinders are assumed to have equal adsorptive areas.

Recently the adsorption of cyclohexane and benzene on nickel, iron and their oxides have been measured (Barbernics Tertenyi and Kertesz 1974). Using this data to obtain N^{o} (taken as 4.5×10^{-6} mol m^{-2}), assuming that the adsorptive area of each cylinder was the geometric area (0.3 m^{2}), C = 100 and using equations (3.55, .56 and .57), the variation of $\delta\varepsilon$ with P/P^{o} was investigated. The results are illustrated in figure 3.4.

The sensitivity of this calculation to the isotherm parameter (figure 3.5) and adsorptive area (figure 3.6) was also studied.

3-6.3 Capillary Condensation

The third possibility of losing or gaining moles of vapour during the experiment is capillary condensation.

If, due to the existence of small superficial cracks in the cylinders, the saturation vapour pressure was lowered, then, after mixing,the partial pressure of each component is halved and so any condensed vapour would then revaporize.

If we have a capillary of radius r metres and we assume zero angle of liquid-solid contact, then by a force balance

$$2\pi r\gamma = (P' - P^o)\ \pi r^2 \tag{3.58}$$

where P' is the new, depressed saturation vapour pressure, and γ is the surface tension.

At equilibrium

$$\mu^g(P^o) = \mu^l(P^o) \tag{3.59}$$

and $$\mu^g(P') = \mu^l(P') \tag{3.60}$$

where μ is the chemical of the gas (g) and the liquid (l).

So

$$\mu^g(P') = \mu^l(P^o) + V^l(P'-P^o)$$

where V^l is the liquid molar volume

$$= \mu^l(P^o) + V^l \frac{2\gamma}{r} \tag{3.61}$$

substituting from equation (3.58)

Since

$$\mu^g(P') = \mu^g(P^o) + RT \ln \frac{P'}{P^o} \tag{3.62}$$

then

$$\ln \frac{P'}{P^o} = \frac{2\gamma V^o}{RTr} \tag{3.63}$$

Now, our loading pressures are about 0.6 P^o or less, and so equation (3.63) can be used to determine what sized crack was required to cause capillary condensation.

Using typical organic liquid values at 300 K for $\gamma(2\text{x}10^{-2}$ J $m^{-3})$

and V^1 (10^{-4} m^3) gives

$$r = 3 \times 10^{-9} \text{ m}$$

Cracks of this size are only slightly greater than the size of molecules and so it would be difficult, in our situation, to distinguish between capillary condensation and surface adsorption.

3-7 The Effect of Relative Temperature Shifts in the Equipment

In section 2, the effect of the whole apparatus changing temperature was analysed.

However, if individual items of the apparatus alter temperature relative to each other during the course of an experiment, the measured pressure difference will differ from the pressure difference caused by mixing alone.

Using figure 3.2, we may write for the initial loading of the apparatus

$$PV = n_1RT + n_1B_{11}P \tag{3.1}$$

and $$PV = n_2RT + n_2B_{22}P \tag{3.2}$$

After mixing,

$$P_m = (n_1 + n_2)RT + (n_1 + n_2)B_m \tag{3.3}$$

For the reference cylinder, after it has been isolated, we have

$$PV_r = n_rRT + n_rB_{11}P \tag{3.64}$$

where the subscript r refers to the reference vessel.

Now if the temperature between the reference cylinder and the mixing cylinders alters by δT, then the corresponding change in the reference pressure δP is given by

$$(P+\delta P)V_r = n_rR(T+\delta T) + n_rB_{11}(P+\delta P) \tag{3.65}$$

assuming that the δB also caused is negligible. Equations (3.65 and .64) give

$$\frac{\delta P}{P} = \frac{\delta T}{T} \tag{3.66}$$

after some rearrangement.

Now P_m will be given by

$$P_m = P + \Delta P + \delta P \qquad (3.67)$$

Using this relationship and rearranging equations (3.1, .2 and .3) as in previous sections gives

$$B_m - x_1 B_{11} - x_2 B_{22} = \frac{RT}{P}\left(1 - \frac{1}{1 + \frac{\Delta P}{P} + \frac{\delta P}{P}}\right)$$

$$\text{i.e.} \quad 2x_1 x_2 \epsilon = \frac{RT}{P}\left(\frac{\Delta P}{P} + \frac{\delta P}{P}\right)\left(\left(1 + \frac{\Delta P}{P}\right) + \frac{\delta P}{P}\right)^{-1}$$

$$= \frac{RT}{P\left(1 + \frac{\Delta P}{P}\right)}\left(\frac{\Delta P}{P} + \frac{\delta P}{P}\right)\left(1 + \frac{\delta P}{P+\Delta P}\right)^{-1}$$

$$= \left[\frac{RT\Delta P}{P^2\left(1 + \frac{\Delta P}{P}\right)} + \frac{RT\delta P}{P^2\left(1 + \frac{\Delta P}{P}\right)}\left(1 - \frac{\delta P}{P+\Delta P}\right)\right]$$

since δP is small compared with P.

i.e.

$$2x_1 x_2 \epsilon = 2x_1 x_2 \epsilon_{\text{apparent}} + \frac{RT\delta P}{P^2\left(1 + \frac{\Delta P}{P}\right)} + \text{terms in } \frac{\delta P}{P^3} \qquad (3.68)$$

$$\text{so} \quad \delta\epsilon \simeq \frac{RT\delta P}{2x_1 x_2 P^2\left(1 + \frac{\Delta P}{P}\right)} \qquad (3.69)$$

If, for a loading pressure of 20,000 Pa, $x_1 = x_2 = 0.5$, a δT of 0.001 K will produce an error of 10^{-6} m^3 mol^{-1}.

With a temperature controller capable of sensing 0.002 K, large thermal masses of the cylinders and vigorous thermostat stirring relative temperature drifts of 0.001 K could easily be possible, and so an error of $\pm 10^{-6}$ m^3 mol^{-1} is significant compared with the experimental measurement errors.

3-8 Dynamic Response of the Equipment

By performing an energy balance over the equipment, the response of the apparatus to temperature fluctuations can be estimated. Two sorts of temperature fluctuations are of interest: periodic fluctuations and the return of the equipment to the thermostat temperature after a major temperature disturbance (i.e. after using liquid air in the cold finger).

Performing the energy balance over the surface of the cylinder (see figure 3.7) gives

Energy In: $(UA)_{cf}(T_{cf} - T_g)$

Energy Out: $(UA)_{cy}(T_g - T_o)$

Energy accumulation: $V\rho C_p \frac{dT_g}{dt}$

i.e. $$V\rho C_p \frac{dT_g}{dt} = (UA)_{cf}(T_{cf} - T_g) - (UA)_{cy}(T_g - T_o) \qquad (3.70)$$

where U is the overall heat transfer coefficient (W m^{-2} K^{-1})

A is the surface heat transfer area (m^2)

T is the temperature (K)

V is the cylinder volume (m^3)

ρ is the vapour density (kg m^{-3})

C_p is the specific heat of the vapour at constant pressure (kJ kg^{-1} K^{-1})

and t is the time (s).

The subscripts cf refer to the cold finger, cy the cylinder, g the vapour, and o the oil.

To estimate the response of the vapour temperature to oil temperature fluctuations, we can simplify equation (3.70), assuming that $T_{cf} = T_g$, so

$$\tau \frac{dT_g}{dt} + T_g = T_o \qquad (3.71)$$

where $$\tau = \frac{V\rho C_p}{(UA)_{cy}} \qquad (3.72)$$

If the oil temperature is fluctuating ΔT_o K in a sinusoidal form, i.e.

$$\Delta T_o = \alpha \sin \omega t \qquad (3.73)$$

where α is the amplitude of the fluctuations (K) and

ω is the frequency (s^{-1}),

then the vapour temperature response will be

$$\Delta T_g = \frac{\alpha}{\sqrt{1+\omega^2\tau^2}} \sin (\omega t + \tan^{-1}(-\omega\tau)) + \frac{\alpha\omega\tau}{1+\omega^2\tau^2} e^{-t/\tau} \qquad (3.74)$$

The attenuation factor is $\frac{1}{\sqrt{1+\omega^2\tau^2}}$. So, for our experimental set-up, $V = 6\times10^{-3}$ m^3, $A = 0.3$ m^2, $\rho = 5\times10^{-3}$ kg m^{-3}, $C_p = 2$ kJ kg^{-1} K^{-1}, and $U = 10^{-4}$ W m^{-2} K^{-1} (from experimental measurements) gives

$\tau \simeq 30$ minutes.

Hence, for high-frequency fluctuations, such as turbulence eddies with periods of less than 1 sec, the attenuation factor is 10^{-4}. Low-frequency fluctuations with periods of 300 seconds, such as bulk thermostat temperatures, the attentuation factor is 0.03.

These results indicate that the vapour temperature is insensitive to rapid oil temperature fluctuations and small bulk thermostat movements.

The other case of interest is the time required for the vapour to reach the thermostat temperature after sublimating from the cold finger.

Assuming that the cold finger is at the oil temperature, then equation (3.70) becomes

$$\tau \frac{dT_g}{dt} + (\frac{A_{cf}}{A_{cy}} + 1)\, T_g = (\frac{A_{cf}}{A_{cy}} + 1)\, T_o \qquad (3.75)$$

Since $A_{cf} \simeq 0.01\ A_{cy}$, this becomes

$$\tau \frac{dT_g}{dt} + T_g = T_o \qquad (3.76)$$

The response of the vapour temperature to warming is

$$T_g = T_{g(t=o)} + (T_o - T_{g(t=o)})(1 - e^{-t/\tau}) \qquad (3.77)$$

For τ= 30 minutes as before, and $T_{g(t=o)} = 5^oC$, with $T_o = 50^oC$, then T_g is within 10^{-2} K of T_o after about 4 hours.

CHAPTER 4 EXPERIMENTAL PROCEDURES

This chapter details the chemical preparation used in the measurements as well as giving a detailed experimental procedure description.

4-1 Preparation of the Components

Benzene and cyclohexane from the May and Baker range of chemicals were used.

The cyclohexane specifications were 95% distilling between 80 and 81°C with less than 0.005% residues on complete evaporation. The refractive index at 20°C was claimed to be between 1.425 and 1.427.

The benzene specifications were 93% distilling over 0.25°C range and all distilled between 79.5 and 80.5°C leaving less than 0.002% residues. The toluene and thiophen levels were to be less than 0.05% each.

These chemicals were analysed on a gas chromatograph using a Carbowax column running at 100°C. The chromatograms gave single peaks and no impurities greater than 0.1% were detected.

The 50 to 60 ml of sample to be degassed was loaded into the bulk ampoule (see fig. 4-1) and shaken with 5A molecular sieve, manufactured by Union Carbide Ltd, and regenerated as specified by Union Carbide in our laboratory. This was then left to stand overnight.

With taps T2-T7 open, and T1 shut, the demountable "Soveril" joint J1 was made and tested for leak-tightness to a 0.1 Pa vacuum.

When this vacuum was attained, a freezing mixture of acetone-methanol and dry ice was poured into the primary degasser. A vacuum flask of hot water (70-80°C) was placed around the bulk ampoule and tap T1 slowly opened and set so that the system pressure did not rise above 10 Pa. Once the bulk ampoule was almost dry, taps T1 and T2 were shut and pumping of the frozen sample was continued for 1 to 2 hours, to remove any further gases.

Tap T3 was then closed and liquid air put into the secondary degasser once the dry ice-acetone mixture had been removed from the primary degasser. An infra-red lamp was used to aid the sublimation. When the transfer was complete, tap T3 was opened and the degassers were evacuated to 0.01 Pa. Then the primary degasser was loaded with liquid air and the secondary degasser was warmed, again using an infra-red lamp.

Upon completion of the transfer, the sample was pumped for a further

two hours. Pressures of less than 0.01 Pa were usually obtained. Tap T5 was then closed and either of taps T6 or 7 was closed. An ice-water mixture was then put around the open ampoule and the primary degasser warmed. When the transfer was complete, tap T6 or 7 was closed and T5 opened to allow evacuation of the system prior to degassing the next sample.

4-2 Outline of Experimental Measurement

As shown in Chapter 3, the measurement of ε, where

$$\varepsilon = B_{12} - \frac{1}{2}(B_{11} + B_{22})$$

$$\simeq \frac{2RT\Delta P}{P^2}$$

requires the measurement of three variables, namely

(i) the initial loading pressure of the system (P),

(ii) the temperature of the experiment (T), and

(iii) the change in pressure (ΔP), after the mixing, of the two components when the equipment has returned to the initial temperature.

These three measurements are made by the following sequence (referring to fig. 4-1).

The first component is transferred into cylinders MIX1 and REF, isolated, and allowed to come to thermostat temperature. Dry nitrogen is then admitted via valve V7, to zero the differential pressure transducer, and back-pressure the mercury manometer. This gives the initial loading pressure (P).

The nitrogen is evacuated and valve V6 closed. Component two is then admitted to cylinder MIX2 and the amount adjusted until the pressure transducer again reads zero. Once the REF cylinder has been isolated, to provide the reference pressure for the differential pressure transducer, the valve V3 is opened and the contents of cylinders MIX1 and MIX2 are mixed. When the equipment has returned to the thermostat temperature, the reading of the pressure transducer gives the change in system pressure on mixing (ΔP).

4-3 Detailed Procedure for the Measurement

Each determination of the pressure change on mixing was carried out using the following procedure (refer to fig. 4-1).

(1) All the taps and valves were initially open. The whole apparatus was evacuated to below 0.05 Pa for at least twelve hours. The pressure transducer was adjusted and zeroed. The thermostat temperature was noted and the temperature controller set.

(2) (t = 0) Valves V2, 3 and 5 were closed and liquid air put into the cold finger of cylinder MIX1. With tap T9 closed, an estimated amount of the first component was allowed to evaporate from the sample ampoule to sublime on to the cold finger.

(3) (t = 0.5 hr) Valve V1 was closed. The remaining liquid air in the cold finger was removed and the cold finger warmed by compressed air heated almost to thermostat temperature (see section 5-8). Tap T9 was opened to evacuate the sample supply line.

(4) (t = 1.5 hr) Valve V2 was opened and tap T9 closed. An excess of component two required to balance the pressure in MIX1 was transferred into cylinder MIX2 by adding liquid air to the cold finger.

(5) (t = 2.0 hr) Valve V2 was closed, tap T9 opened to evacuate the supply line and the cold finger unfrozen and warmed to the thermostat temperature.

(6) (t = 6 hr) Tap T11 was closed. Dry nitrogen was admitted to the pressure transducer and the mercury manometer by the needle valve V7 after opening the shut-off valve V8 until the pressure transducer was zeroed or brought to within 130 Pa of the pressure in REF and MIX1. The pressure on the mercury manometer was then measured. Once the pressure had been measured, valve V8 was closed and tap T11 opened to evacuate the nitrogen from the system.

(7) (t = 7 hr) Once the evacuation of the nitrogen was completed, valve V6 was closed and valve V5 opened. Tap T8 was opened and tap T9 was

closed. Liquid air was put around the cold finger under the Penning gauge (fig. 4-1) and valve V2 was used to bleed the excess of component 2 from MIX2 until zero pressure differential was indicated on the transducer.

(8) (t = 8 hr) Since all three cylinders were at nearly the same pressure, valve V3 was opened and the pressure transducer allowed to settle. Then valve V4 was very carefully closed and the reading on the pressure transducer noted. This was the zero difference reading.

(9) (t = 8½ hr) Valve V5 was closed and liquid air poured into one of the cold fingers of MIX1 or 2.

(10) (t = 9 hr) The frozen cold finger was heated back up to near thermostat temperature, as before, and allowed to come to thermal equilibrium.

(11) (t = 10 hr) Valve V5 was opened.

(12) (t = 13 hr) The pressure transducer reading was taken once the value remained constant for several hours.

(13) (next day) The samples were distilled out of the cylinders by putting liquid air in the secondary degasser. When this was complete, all the taps and valves were opened and the system evacuated in preparation for the subsequent run.

CHAPTER 5 EXPERIMENTAL EQUIPMENT

In this chapter, the individual items of equipment that together form the apparatus will be detailed.

Each section will cover, where applicable, the design, materials and methods of construction, the tests used to prove the item's integrity and the operation of each item.

5-1 Vacuum Pumps

The backing pump was an off-the-shelf item from Associated Electrical Industries, Manchester, England. It was a conventional oil-sealed rotary pump, type 6DR1, with a pumping speed of 100 litres/minute. It was capable of achieving a system pressure of 0.1 Pa when cold-trapped.

The mercury vapour diffusion pump was designed and built, in glass, by Mr F. Downing of the Chemistry Department. It was a conventional, two-stage, umbrella type pump. The pump contained about a kilogram of mercury and was heated electrically, consuming 200 to 250 watts.

When cold-trapped with liquid air, the rotary and diffusional pumps were capable of reducing the whole experimental system to nearly 10^{-4} Pa over a period of days, 10^{-2} Pa being achieved within 24 hours.

5-2 Vacuum Lines, Taps and Ampoules

The vacuum lines were all, except the cylinders and valves, made of "Pyrex" glass. After glass-blowing, the line was evacuated and the joints were tested using the electrical arc from a high-tension coil tester.

Taps T10 to T17 (see fig. 4-1) were conventional ground-glass stopcocks with vacuum grease sealing. The cold-traps were demountable, the ground-glass joints also being grease sealed.

Taps T1 to T9 were 10 mm bore "Young's Taps", manufactured by J.F. Young of Acton, England. These taps were constructed of "Pyrex" glass and "teflon" O-rings were used for the seat and barrel seals. The barrel seal was backed (on the atmospheric side) by a second "Viton" O-ring. These taps were capable of maintaining a 10^{-2} Pa vacuum easily , across the seat and the barrel (as shown by a Penning gauge), for periods of up to 2 to 3 weeks.

The bulk and storage ampoules (see fig. 4-1) were made from "Pyrex" glass tube and "Young's Taps".

The vacuum gauges on the vacuum lines were Edwards Vacuum Pirani 11, with a M6B head, and Penning 8, with a model 6 head. The Penning was used to calibrate the high vacuum end of the Pirani scale.

The demountable joint J1 (see fig. 4-1) was a "Soveril" teflon joint. It consisted of the ends of the lines with a screw thread formed on the outside of each. The composite silicon rubber, "teflon" coated washer was then clamped by an outer screwed sleeve. This joint was capable of maintaining a 0.1 Pa vacuum for 2 to 3 hours.

5-3 Sample Degasser

The degassers were developed along the lines suggested by Battino et al (May 1971) and Bell et al (Dec. 1968).

The dimensions and configurations used are set out in fig. 5-1. Both degassers were made of "Pyrex" glass. The outer dimension was fixed by the availability of glass tubing and the length determined by the sublimate film thickness and size of sample to be degassed. 50 to 100 ml samples were large enough for our uses and a solid thickness of 2 mm was chosen arbitrarily. Later operation showed that this film was not too thick as the vapour losses were very small.

The allowable volume of the degasser was determined by the maximum allowable level of inert gases and the operating pressure whilst degassing as outlined in Chapter 3, section 4.

The gas-vapour flow pattern in the degasser was visualized by bleeding moist air through the degasser when the freezing mixture was loaded. The fog that formed showed a vigorous swirling pattern spiralling up the chamber. Subsequent operation with vapours gave a very even continuous film over the entire cold surface.

5-4 Mercury Manometer

A mercury U-tube manometer was used to measure the initial loading pressure of each experimental run.

The manometer was constructed of 25 mm i.d. Veridia bore tubing to minimize capillary surface effects. The mercury used had been thoroughly washed with NaOH solutions to degrease it, HNO_3 solutions to remove any

non-noble metals, then distilled under vacuum to separate out any noble metal contaminants. Finally the purified mercury was dried by passing filtered, dried air through it.

Once this sequence had been completed, the mercury was loaded into the manometer under vacuum.

The mercury levels were measured using a Precision Tool and Instrument Company cathetometer No. 17407.

The mercury surfaces were back-lit by two 900 mm 20 watt fluorescent tube lights. Brass collars to hood, and so collimate the light from, the mercury surface were used.

The whole manometer was enclosed in a cabinet lined with 10 mm polystyrene sheet so that air draughts around the manometer were minimized. A 50 mm slit in the front of the cabinet allowed the mercury levels to be sighted by the cathetometer.

The cathetometer was sited so that the vertical measuring bar was equidistant from the manometer legs. This made sure that the telescope was at the same distance from either manometer leg (since the bar was the pivoting point) and hence made sure that no refocussing of the telescope was required. Before each set of pressure measurements, the measuring bar was checked for vertical alignment using the spirit-level on the telescope. This ensured that no relevelling of the telescope was required between individual readings.

5-5 The Differential Pressure Transducer

The differential pressure transducer used was a commercial model (MKS "Baratron") available from M.K.S. Instruments Inc. of Burlington, Massachusetts, U.S.A. The instrument consisted of a Type 90M-XR Indicator, serial No. K5106, and a Type 90 Pressure Head, Type 90H-1E, serial No. K5197, full-scale deflection of 130 Pa (1 mmHg).

The transducer was of the variable capacitance type (see fig. 5-2), i.e. the diaphragm forms the common plate of two variable capacitors back

to back. The movement of the diaphragm alters the capacitance in an oscillator circuit, hence altering the resonant frequency. This frequency is then compared with a fixed frequency oscillator and the variation calibrated in terms of the pressure difference being measured.

The MKS Company provided this calibration. The calibration was done using an air-dead-weight gauge, with a claimed resolution of 1.3×10^{-4} Pa (10^{-6} mmHg).

The sensor-head was constructed of Inconel with an Inconel "X" diaphragm. The pressure tappings were made of 304 stainless steel. The capacitor electrodes were fused in place with high-temperature ceramics. Cajon fittings of 316 stainless steel were used to join the transducer to the mixing cylinder assembly.

The transducer was fitted with a close-fitting mild steel shell to allow the sensing head to be completely immersed in the thermostat oil. The shell flange was sealed with silicon sealant and the interior filled with fibre-glass insulation. A snorkel was used to lift the triaxial cables from the sensor, out of the bath, to the preamplifier. This snorkel was also packed with fibre-glass to prevent induced cooling that might be caused by any free-convection with the room.

The 50, 20 and 3 Pa readings of the Baratron were checked and found to agree with a McLeod gauge using dry nitrogen. The resolution of the McLeod gauge was ±1%. The McLeod gauge was of the fixed compression ratio type. The capillary and bulb volumes were found using weighed amounts of mercury and water. The pressure head was determined by using a cathetometer to measure the mercury levels.

5-6 High-pressure Nitrogen Supply

The high-pressure nitrogen used to back-pressure the pressure transducer and mercury manometer (see fig. 4-1) was oxygen-free dry nitrogen supplied by New Zealand Industrial Gases Ltd. The nitrogen was throttled using a NZIG reducing regulator (V9) and passed through a bed of dry silica-gel. The

nitrogen was then passed through a shut-off valve (V8) to an "Edwards Speedivac" needle valve (type OS1C), from which the flow of nitrogen to the transducer and manometer was controlled. The whole assembly was safe-guarded against over-pressure by a mercury blow-down valve vented to the atmosphere.

5-7 Mixing Cylinders and Assembly

The three mixing cylinders were 6 litre, 316 stainless steel vessels 150 mm in diameter, 360 mm deep (see fig. 5-3), all joints being argon-arc welded. Each cylinder had a 10 mm dia. entrance tube made from copper. Two of the cylinders had re-entrant cold fingers in place.

"Hoke"valves (model 4618N4) were used for the valve assembly (see fig. 5-4). The monel metal valves were welded into the brass joining pieces with bronze to make a complete subassembly which was then thoroughly washed with acetone and water. This valve assembly was then joined to the cylinder assembly using 220^{o}C melting point solder. No flux was used when making this final seal. The pressure transducer was then bolted to the valve assembly by the "Cajon" fittings.

The complete assembly of valves and cylinders was then mounted into the thermostat support frame and the glass-metal seals joined into the vacuum system.

The cylinders and valves were thoroughly washed, cleaned and degreased using NaOH, HCl and HNO_3 washes, each wash being followed by thorough rinsing with distilled water. Further cleansing was done using distilled trichloroethane degreaser followed by redistilled acetone washes.

The cylinders were then electropolished at a current density of 150-200 amp/m^2 at 10-20 volts for 20-30 minutes. The polishing solution consisted of 30% H_3PO_4, 45% H_2SO_4, 5% Na_2CrO_4 in water. The electropolishing was followed by prolonged washing in distilled water.

Each cylinder and the valve assembly was leak-tested using a Texas Instruments "Minimass" spectrometer with H_2 as the tracer gas. System test

pressures of better than 10^{-4} Pa were obtained for these tests. No H_2 was detected in any of the assemblies under test.

Finally, each cylinder, the valve assembly and the pressure transducer were baked in an oven under a vacuum of 0.1 Pa or better. The cylinders and pressure transducer were held at 400°C for 3 to 4 hours, this being the time required to attain that temperature. The valves, because of their temperature limitation of 310°C, were baked for a similar period to the cylinders at 300°C.

5-8 Thermostat

The thermostat consisted of a 150 litre steel tank, 600 mm x 500 mm x 600 mm deep, insulated with 25 mm of fibre-glass. BP TH65HB oil was used for the bath fluid as it would stand temperatures of 150°C. This oil has a vapour flash-point of 220°C.

Stirring in the bath was done by a single six-bladed propellor powered by a 300 watt motor. This gave vigorous fluid movement and any temperature variation was reflected throughout the bath in 2 to 5 seconds.

Heating of the bath was done by two heaters, a 1 kW immersion heater and a "pyrotenax" heater of 800 W. The immersion heater was rated at 5 kW but was only used to a 1 kW limit to prevent oil charring due to a high heat flux at the element surface. This heater was only used to change the thermostat temperature.

The 800 W "pyrotenax" heater consisted of 35 metres of "pyrotenax" wire on a former surrounding the cylinders. This heater was used as the controlled heater. Bath temperature control was achieved by using a S.C.R. proportional temperature controller (Martin) with an appropriate thermistor immersed in the oil as the sensor. The controller responded to temperature variations of ±0.001°C and controlled the bath temperature to ±0.01 °C over 20 minutes as measured by a Beckman thermometer. The long-term drift, i.e. over 24 hours, was also ±0.01°C.

When required, bath cooling was achieved by passing mains water through 15 metres of 5 mm dia. copper tubing mounted on the same frame as the "pyrotenax" heater. On full flow, this cooler was capable of absorbing over 1 kW of energy from the bath.

Accurate temperature control was maintained by slightly over-cooling the bath and then using the controller to maintain the temperature required.

Several times during each experimental run, the two cold-fingers in cylinders MIX1 and MIX2 had to be emptied of liquid air and heated back to the bath temperature. This was done by passing compressed air through a portable heat-exchanger immersed in the bath and the outlet placed in the bottom of the cold finger.

The heat exchanger consisted of a 1 metre, 10 mm diameter, copper tube coiled into a 50 mm diameter coil and placed in the thermostat. The outlet was then put deep into the cold finger and the compressed air supply turned on. With exit velocities of about 1 m/s out of the cold finger, the flushing air was up to 90% of the bath temperature (in ^{o}C) within 10 to 15 minutes.

5-9 Temperature Measurement

The primary temperature measurement was done with a Rosemount platinum resistance thermometer and comparative bridge. The bridge was a transformer bridge, model VLF51A-150. The platinum transfer head was model WS104, serial number 240.

The resistance thermometer was used when the Beckman thermometer showed that the bath temperature was stable. Then the Beckman was used as a check on the long-term temperature drift.

CHAPTER 6 EXPERIMENTAL RESULTS AND CALCULATIONS

6-1 Calculation Details

The results tabulated in Table 6-1 were calculated using a truncated form of equation (3.9), namely

$$\varepsilon = \frac{2RT\Delta P}{P^2(1+\frac{\Delta P}{P})} \qquad (3.9)$$

The $2x_1x_2$ term has been approximated to 0.5 as the deviation of the x_1x_2 product from 0.25 was never greater than 6 parts per million for the loading pressures used (determined from equations 3.1 and 3.2).

As illustrated in Chapter 3-2, the major source of measurement error is in the ΔP term. The relative error here is ten times greater than in the x_1x_2, P or T terms. Hence the error quoted for ε in Table 6-1 is error caused by the uncertainty in the ΔP measurement.

The absolute pressure measurement was obtained by using a mercury manometer and cathetometer. These measurements were then corrected to 273 K using mercury density-temperature data (Weast 1970). The value of $g = 9.81\ m\ s^{-2}$ was used to convert the mercury reading into pascals.

The temperature was determined with a platinum resistance thermometer as outlined in Chapter 5.

The value of $R = 8.3144\ J\ mol^{-1}\ K^{-1}$ was used throughout, for the universal gas constant.

A set of results, obtained when the apparatus was contaminated with oil (we suspect), is presented in Appendix IV. The errors quoted are, again, measurement errors determined from the ΔP measurement.

6-2 Raw Data and Calculated Results

Table 6-1 MEASUREMENT DATA AND CALCULATED RESULTS

Run No.	Temperature K ±0.01 K	Loading Pressure Pa ±10 Pa	Pressure Change Pa	Excess Virial Coefficient $m^3\ mol^{-1}/10^{-6}$	Reference Component
25	300.00	9,310	2.5±0.1	144±6	Benzene
26	"	9,810	4.7±1.0	244±52	Cyclohexane
31	315.16	10,770	0.46±0.07	21±3	Cyclohexane
32	"	9,380	0.14±0.07	8±4	Benzene
33	"	16,180	2.44±0.07	49±2	Cyclohexane
34	"	17,080	1.60±0.07	29±1	Benzene
35	"	6,080	-0.26±0.07	-37±10	Benzene
23	323.16	22,760	4.06±0.1	42±1	Benzene
24	"	23,330	4.35±0.1	43±1	Cyclohexane
29	348.16	29,810	2.3±0.2	15±1	Cyclohexane
30	"	26,140	1.9±0.2	16±2	Benzene
27	373.16	38,290	4.0±0.4	17±2	Benzene
28	"	43,250	6.0±0.4	20±2	Cyclohexane

6-3 Results Corrected for Adsorption

The results of Table 6-1 have been adjusted assuming a correction due to adsorption is required and presented in Table 6-2 and figure 6.1. The correction was done using figure 3.4. The percentage of saturation vapour pressure for the loading pressure was determined and the correction read off directly.

The error assigned to ε was either the corrected spread of results or the measurement error, whichever was the larger.

Table 6-2 RESULTS CORRECTED FOR ADSORPTION

Run No.	Temperature K ±0.01 K	Loading Pressure Pa ±10 Pa	Fraction of Saturated Vapour Pressure	Excess Virial Coefficient $\delta\varepsilon_{Adsorption}$ (from Fig.3.3) $m^3 mol^{-1}/10^{-6}$	$\varepsilon_{uncorrected}$ $m^3 mol^{-1}/10^{-6}$	$\varepsilon_{corrected}$ $m^3 mol^{-1}/10^{-6}$
25	300.00	9,310	0.70	-10	140±6	130
26	"	9,810	0.74	-20	240±50	220
					ε_{300} = 175±50	
31	315.16	10,770	0.40	+20	21±3	41
32	"	9,380	0.35	+28	8±4	36
33	"	16,180	0.61	+5	49±2	54
34	"	17,080	0.64	+1	29±1	30
35	"	6,080	0.23	+65	-37±10	28
					ε_{315} = 38±16	
23	323.16	22,760	0.63	+2	42±1	44
24	"	23,330	0.64	+1	43±1	44
					ε_{323} = 44±1	
29	348.16	29,810	0.36	+3	15±1	18
30	"	26,140	0.31	+4	16±2	20
					ε_{348} = 19±3	
27	373.16	38,290	0.21	+3	17±2	20
28	"	43,250	0.24	+2	20±2	22
					ε_{373} = 21±3	

6-4 Comparison with Literature Values for the Excess Virial Coefficient

Table 6-3 A COMPARISON BETWEEN THE LITERATURE VALUES AND THIS WORK, OF THE EXCESS SECOND VIRIAL COEFFICIENT OF BENZENE AND CYCLOHEXANE

T/K	ε / $m^3\ mol^{-1} \times 10^{-6}$	Source
298	135±80	Knobler and Pasco (1975)
300	175±50	This work
313	30±45	McElroy (1968)
315	38±16	This work
318	45±20	McElroy (1968)
323	35±10	McElroy (1968)
	44±1	This work
333	14±15	McElroy (1968)
348	19±3	This work
373	21±3	This work
	18±2	Knobler and Pasco (1975)

The results presented in Table 6-3 are illustrated in figure 6.2.

6-5 Second Virial Coefficients of Benzene and Cyclohexane

The table of values for the second virial coefficients of benzene and cyclohexane, presented in Table 6-4, have been taken from Dymond and Smith (1968). These values represent the best curve through the best existing data (105 points for benzene, 30 points for cyclohexane). The errors quoted represent their estimate of the uncertainty in the smoothed values.

Chan (1976) has determined a least squares fit to these smoothed data, taking the experimental errors into account, using the McGlashan and Potter corresponding states relationship:

$$\frac{B}{V_c} = 0.43 - 0.886 \frac{T_c}{T} - 0.694 \left(\frac{T_c}{T}\right)^2 - 0.0375(n-1)\left(\frac{T_c}{T}\right)^{4.5} \qquad (1.18)$$

where B is the second virial coefficient in $m^3\ mol^{-1}$

T is the temperature in K

T_c is the critical temperature in K

V_c is the critical molar volume in $m^3\ mol^{-1}$

and n is a molecular parameter.

Chan's (1968) results and critical data are presented in Table 6-4a. The function together with the smoothed data points and their errors are illustrated in figure 6.3.

An alternative procedure using a modified Pitzer-Curl correlation (Tsonopolous 1974) was also tried, i.e.

$$\frac{BP_c}{RT_c} = f(o) + \omega f(1) \qquad (6.1)$$

where $f(o) = 0.1445 - 0.33 \frac{T_c}{T} - 0.1385 \left(\frac{T_c}{T}\right)^2 - 0.0121 \left(\frac{T_c}{T}\right)^3 - 0.000607 \left(\frac{T_c}{T}\right)^8$ (6.2)

$$f(1) = 0.0637 + 0.331 \left(\frac{T_c}{T}\right)^2 - 0.423 \left(\frac{T_c}{T}\right)^3 - 0.008 \left(\frac{T_c}{T}\right)^8 \qquad (6.3)$$

and P_c is the critical pressure.

The results, using the accentric factors derived from vapour pressure data ($\omega_{benzene} = 0.211$ and $\omega_{cyclohexane} = 0.209$) are shown in figure 6.3 also.

Table 6-4 THE SECOND VIRIAL COEFFICIENTS OF BENZENE AND CYCLOHEXANE

(from Dymond and Smith 1968)

BENZENE	T/K	$\frac{B}{m^3\ mol^{-1} x10^{-6}}$
	300	-1460±50
	320	-1220±50
	340	-1060±40
	360	-920±40
	380	-810±40
	400	-700±30
CYCLOHEXANE	310	-1500±50
	320	-1370±50
	330	-1260±50
	340	-1170±50
	350	-1080±50
	360	-1000±50
	370	-900±50
	380	-820±50

Table 6-4a BEST FIT OF THE McGLASHAN-POTTER EQUATION TO THE SMOOTHED VALUES OF BENZENE AND CYCLOHEXANE

	Benzene	Cyclohexane
T_c/K	562	553
$V_c/m^3\ mol^{-1}$	$2.604x10^{-4}$	$3.08x10^{-4}$
n	4.07	3.83
Sums squared deviation	$2.6x10^{-8}$	$4.8x10^{-8}$

6-6 Comparison with Literature Values for the Interaction Virial Coefficients of Benzene-Cyclohexane

Table 6-5 sets out, and figure 6.4 illustrates, the comparison of the interaction second virial coefficient (B_{12}) of benzene-cyclohexane with temperature.

The errors for the values of Knobler and Pasco, McElroy and this work have been calculated by averaging the pure component errors and adding the excess virial coefficient error.

The errors assigned to the determinations of Bottomley and Coopes, Cox and Stubley and Waelbroeck are much larger than they quote as their assumed errors in the pure component values were very optimistic. These errors have been recalculated by adding to the average of the Dymond and Smith pure component errors twice the quoted error in B_m. Twice the quoted error was used as these values were determined from the mixture virial coefficients, i.e. for a 50-50 mixture

$$B_{12} = 2B_m - \tfrac{1}{2}B_{11} - \tfrac{1}{2}B_{22} \qquad (6.4)$$

and, in all cases, the mixture coefficient was quoted to about $\pm 10 \times 10^{-6}$ $m^3\ mol^{-1}$.

Table 6-5 A COMPARISON BETWEEN THE LITERATURE VALUES AND THIS WORK OF THE INTERACTION SECOND VIRIAL COEFFICIENT OF BENZENE AND CYCLOHEXANE

T/K	B_{12} / $m^3\ mol^{-1} \times 10^{-6}$	Source
298	-1410±130	Knobler and Pasco (1975)
300	-1355±100	This work
308	-1346±70	Bottomley and Coopes (1962)
313	-1336±95	McElroy (1968)
315	-1340±60	This work
318	-1272±70	McElroy (1968)
323	-1225±50	This work
	-1222±60	McElroy (1968)
	-1215±70	Bottomley and Coopes (1962)
328	-1227±70	Waelbroeck (1955)
333	-1144±65	McElroy (1968)
	-1203±70	Waelbroeck (1955)
343	-1041±70	Bottomley and Coopes (1962)
	-1109±70	Waelbroeck (1955)
348	-1075±70	Waelbroeck (1955)
	-1035±47	This work
373	-910	Cox and Stubley (1960)
	-844±47	This work
	-844±47	Knobler and Pasco (1975)

7-1 Accuracy of the Excess Interaction Measurement and the Experimental Technique

The four subsections of this first part of the discussion will deal with the advantages of the measurement technique we have developed, along with a discussion of the resulting measurement errors. Finally, the development of the adsorption and absorption models will be discussed.

7-1.1 The "Open Tap" Technique

The "open-tap" technique is so called because after the cylinders MIX1 and MIX2 (see figure 4.1) have been loaded and balanced, valves V3 and V5 are opened, the pressure fluctuations allowed to settle, and then valve V4 is gently closed. The reading on the pressure transducer is the zero pressure difference reading. Before mixing is induced by pouring liquid air into one of the cold fingers, the valve V5 is closed. Then, when the mixture is frozen, the pressure transducer is not subject to an overload deflection. After the mixture has been returned to the thermostat temperature, V5 is then opened and the pressure change measured. By this means, the effect of volume changes caused by opening and shutting the valves is avoided and, in this case, more importantly, the likelihood of a transducer zero shift is greatly reduced. The zero shift may also be checked by opening valve V4 once the measurement has been completed. In practice, we found that the zero pressure difference reading before and after the mixing never varied by more than 0.01 Pa ($\simeq 10^{-1}$ torr).

Since, before mixing, the two cylinders were almost at the same pressure, opening valve V3 before inducing mixing had little effect as the pressure difference was too small to cause any significant mixing. Further mixing would be caused by diffusion. Since obtaining the zero pressure difference reading never took longer than 10 minutes, usually taking only 5 minutes, this effect was not detected. The amount of vapour left unmixed in the pipe beyond valve V5 and in the diaphragm chamber, again was not large enough to affect the measurement, as the pressure difference on mixing is dependent on the mole fraction product only.

An important design development of the cold fingers was the provision of cups at the bottom of the cold finger. This was done to prevent liquid dripping off the end on to the hot surface of the cylinder wall and revaporizing. In this manner, the energy transfer rate, caused by the mass recycle, was greater than could be removed by the evaporation of liquid air. The result was that it was very difficult, if not impossible, to freeze the cold fingers with vapour present in the cylinders. With the addition of the liquid cups, and increasing the cold-finger diameter to 35 mm, no further problem was experienced.

Another effect that caused larger pressure difference fluctuations than we initially expected was the fluctuations caused by the thermostat controller altering the power input into the oil to maintain the required temperature. This had the effect of altering the residual temperature difference between the cylinders. This in turn caused a pressure difference change. On testing this effect, very small alterations of the controller set point (of the order of thousandth's K) caused pressure difference fluctuations of 0.1 Pa. This was very noticeable with a controller able to sense a thousandth K and a differential pressure transducer with a resolution of better than 0.01 Pa.

The problem was partially overcome by removing the cause of the controller-induced compensations, the room temperature fluctuations. Using an air-conditioning unit and a bias heater, the room temperature was maintained within 0.5 K. To eliminate the effect completely would require more vigorous stirring of the thermostat (300 watts was insufficient in 150 litres), together with another encompassing thermostat controlled to fine limits. Indeed, the inner thermostat should not be controlled at all, relying entirely on the external thermostat. Provided the inner thermostat has a large enough thermal mass, the effect of warming the vapour back to thermostat temperature would not cause lengthy waits. Disadvantages of this system would be the length of time required to alter the thermostat temperature and access to the components of the apparatus.

7-1.2 Measurement Errors

A summary of the error analysis, developed in chapter 3, excluding adsorption or absorption, is shown below in Table 7-1.

Table 7-1 A SUMMARY OF ERRORS: THEIR SOURCES AND LIKELY MAGNITUDE

Source	$m^3\ mol^{-1} \times 10^{-6}$
Measurement (random)	±0.5 to ±5.0
Extrapolation (systematic)	±0.5
Effect of impurities (systematic)	±0.002
Balancing loading pressures (random)	±0.7
Relative temperature drifts (random)	±1.0

As illustrated in the table, the major source of error was likely to be the measurement error. Chapter 3 indicates that the major source of the measurement error is the uncertainty in the pressure difference. The reproduceability of the measurements at 323, 348 and 373 K were all within this pressure difference uncertainty. The loading pressures were able to be balanced to better than ±0.1 Pa in all cases.

The errors likely to be induced by impure vapours of inert gases were not apparent. Different batches of degassed components gave the same answers.

The systematic error caused by the third virial coefficients was estimated in chapter 3 to be $\pm 2 \times 10^{-6}$ m^3 mol^{-1} for a 100 kPa extrapolation to 0 Pa. Since the largest loading pressure used was 40 kPa, with most being about 20 kPa, a systematic error of $\pm 0.5 \times 10^{-6}$ m^3 mol^{-1} has been estimated.

As illustrated in chapter 3-7 and discussed in the previous section, the experiment is extremely sensitive to relative temperature changes between the apparatus components. Hence uncertainties of $\pm 2 \times 10^{-6}$ m^3 mol^{-1} could arise, although we have estimated $\pm 10^{-6}$ m^3 mol^{-1} as being most likely.

Overall, the measurement errors of the excess coefficients are ±2% or $\pm 5 \times 10^{-6}$ m^3 mol^{-1}, whichever is the greater.

7-1.3 Oil-Vapour Absorption

As illustrated in figure 3.3, trace amounts of oil in the apparatus could cause complex and catastrophic effects. The analysis set out in chapter 3-6.1 was developed after the series of experimental runs, listed in appendix IV, was completed. The effects observed disappeared after the equipment was dismantled and baked out to 400+°C at less than 0.1 Pa pressure. This experience graphically demonstrates the level of cleanliness required for the experiment with vapours; a cleanliness beyond the capability of organic degreasers, acid and alkali washes.

As set out in chapter 3-6.1, the effect of oil on the results depends on its position in the apparatus. If one of the mixing cylinders is contaminated, a symmetrical effect becomes apparent, the true result lying mid-way between the results obtained by changing the mixing order. If oil is only present in the reference cylinder, a positive bias in the results occurs.

The extent of each effect depends upon the amount of oil present and the saturation vapour pressures of the two components The two effects together create an unusual pattern due to the interactive nature of the effects. Oil in the reference cylinder would cause too few moles of component 2 to be loaded into cylinder MIX2; this would then skew and enlarge the effect caused by oil in the mixing cylinders.

The results in appendix IV, when compared with the latter results given in table 6-2, follow the trend demonstrated in figure 3.3. The 373 K results are essentially the same with little bias or splay. The results at 323 K indicate both bias and splay, i.e. with benzene as the reference component a correction of $+24 \times 10^{-6}$ m^3 mol^{-1} is required. However, with cyclohexane as the reference component, a correction of $+10 \times 10^{-6}$ m^3 mol^{-1} is needed. At 298 K, corrections of the order of

several hundred $x10^{-6}$ m^3 mol^{-1} seem to be required.

The results of figure 3.3 are not quantitative as, one, we do not have enough results to fit the model accurately and, secondly, oil, being a high molecular weight compound, would be expected to exhibit large negative deviations from the Raoult's law assumption used in the analysis. So the amount of oil is probably even less than the 10^{-7} to 10^{-9} moles we are postulating here.

Also, for the sake of clarity we have used a constant loading pressure, 60% that of the saturation vapour pressure. Altering the loading pressure alters the magnitude of the symmetric effect linearly and the bias inversely. So when comparing the results of appendix IV with figure 3.3 and table 6-2, the bias effect of the 373 K results would be enlarged due to the lower loading pressure, whereas at 298 K the symmetrical effect may be larger than postulated. Again, due to the lack of data, only trends may be observed.

7-1.4 Surface-Vapour Adsorption

The model postulated in chapter 3-6.2, again, can only be used qualitatively. More accurate data on the adsorptive site area of each molecule of either component, how the adsorption of the mixture differs from that of the pure components, but, most importantly, the true adsorptive area of the cylinders is required.

Studies on oxide films indicate that the adsorptive area may be up to ten times the geometric area.

The calculation in chapter 3-6.2 was done using the geometric area of the cylinders. The correction required due to the effect of surface adsorption could be more than ten times greater than this.

The calculation points out two major factors:

(i) The effect is largely insensitive to the B.E.T. isotherm parameter C. For a non-polar adsorber on to a polar substrate, C usually has a value of about 100.

Figure 3.5 shows that values of C, ranging from 50 to 1000, cause relatively minor effects.

(ii) For the type of isotherm postulated, i.e. an isotherm with one inflexion, there will exist a loading pressure that will cause the adsorptive effects to cancel. However, this particular loading pressure would vary with each system and would be very difficult to determine experimentally.

The amount of material that is required to produce the effects postulated here is very small - about 10^{-7} moles. As soon as the total number of moles in the apparatus is less than 10^{-2} moles, the effect becomes very noticeable.

Using the model postulated, as presented in figure 3.4, to correct the results obtained at 315 K, at various loading pressures, produces a dramatic improvement in the spread of the results. The uncorrected results range from -37×10^{-6} m^3 mol^{-1} to 49×10^{-6} m^3 mol^{-1}. Corrected for adsorption, using the geometric area of the cylinders, the results now range from 28 to 54×10^{-6} m^3 mol^{-1}. Increasing the postulated adsorptive area, narrows the spread even further.

Using figure 3.6 to give the adsorptive correction with an adsorptive area twice that of the geometric area of the cylinders produces the following table, table 7-2.

Table 7-2 ADSORPTIVE CORRECTIONS TO THE 315K MEASUREMENTS

(i) ca. Table 6-2
(ii) Adsorptive area = 2 x geometric area
(iii) Corrections from figure 3.6

Run No.	Fraction of Saturated Vapour Pressure	$\delta\varepsilon$	$\varepsilon_{apparent}$	ε
			m^3 $mol^{-1} \times 10^{-6}$	
31	0.40	+40	21±3	61
32	0.35	+56	8±4	64
33	0.61	+6	49±2	54
34	0.64	+2	29±1	31
35	0.23	≃150(estm)	-37±10	≃110

Runs 31, 32 and 33 indicate a value of about 60×10^{-6} m^3 mol^{-1}. Run 34 is consistently low and should be checked. Run 35 resulted in a very small pressure difference, and the correction required is very large, hence it is probably not very reliable. A value of 60×10^{-6} m^3 mol^{-1} is more in keeping with the 323 K result.

Also, further calculations, increasing the adsorptive area still further, indicated that with a factor of 5, corrections at 315 K were enormous, and that sizable corrections would be required for the 373 and 348 K results.

So, a factor of two between the adsorptive and geometric areas seems most likely for our equipment.

The form of the calculated corrections illustrated in figure 3.3 tend to be confirmed by the experimental results. Measurements done at high temperature, where the adsorptive correction is of the same size as the measurement errors, produce consistency, whereas the measurements done at lower temperatures produce highly inconsistent results requiring corrections.

7-2 Comparison of Results with Literature Values

In this section, the excess virial coefficients will be compared and discussed. Then the interaction second virial coefficients will be compared and discussed also. Finally, attempts to predict and correlate both the excess and the interaction second virial coefficients are discussed.

7-2.1 Comparison of Excess Second Virial Coefficients

At 373 K our results agree with those of Knobler and Pasco (1975). However, at the 298-300 K region, the effect of adsorption is very dramatic and largely unquantifiable. Also, our equipment may still be contaminated with oil. Knobler and Pasco's results at 298 K seem to be similarly inconsistent. Both results in the low temperature region appear to be too large, as indicated by the value of the interaction virial coefficient it gives (see figure 6-4).

The results of the 315-350 K region largely agree with those of McElroy

(1968). Our 323 K result seems to be too large when compared with the 315 and 348 K results. This is surprising as the adsorption correction would be expected to be minimal since the loading pressures were close to the 66% of saturation vapour pressure. Alternatively, the adsorption correction applied to the 315 K result may be too small (due to an incorrect adsorptive area) and hence the corrected result is still too small.

Measurements, in our department, of the excess heats of mixing of benzene and cyclohexane at 356 and 323 K tend to confirm the higher temperature results and suggest that the lower temperatures are too positive.

Mayhew (1976) has measured $(H^E/P)_{323} = (21\pm3)\times10^{-5}$ m^3 mol^{-1} and $(H^E/P)_{356} = (5\pm0.4)\times10^{-5}$ m^3 mol^{-1} in a flow calorimeter with a mole fraction of benzene at 0.548 in both cases. Wormald (1969b) measured $(H^E/P)_{373} = (4\pm1)\times10^{-5}$ m^3 mol^{-1}.

Using equation (1.30) and values of ε from figure 6-2, gives $(d\varepsilon/dT)_{323} = -1.2\times10^{-6}$ m^3 mol^{-1} K^{-1}, $(d\varepsilon/dT)_{356} = -2.2\times10^{-7}$ m^3 mol^{-1} K^{-1} and $(d\varepsilon/dT)_{373} = -1.6\times10^{-7}$ m^3 mol^{-1} K^{-1}. These slopes are shown in figures 6-1 and 6-2.

7-2.2 Comparison of the Second Interaction Virial Coefficients

At 373 K our interaction coefficient agrees with that of Knobler. The result of Cox and Stubley appears too negative.

Our results agree with those of Bottomley and Coopes and McElroy down to 320 K. Their 308 K result seems to be too positive, as does Knobler's and ours at 300 K.

Waelbroeck's results are consistently more negative than Bottomley and Coopes', McElroy's and our latest measurements.

As noted in chapter 7, the errors quoted and presented on Bottomley and Coopes and Waelbroeck's results are much larger than they quote due to the larger errors we have used for the pure coefficients. Even these larger errors may not be large enough as the error component in the B_{12} due to the mixture measurement seems to be very optimistic compared with

7-2.3 Correlation of Existing Results

Attempts to arrive at a mixture rule based on the pseudo-alkane concept of Guggenheim-Wormald (1965) fails to correlate the excess coefficients due to the extreme sensitivity of this quantity to the n value. The interaction coefficient is correlated within the experimental errors. However, the experimental errors are still too large to provide a definitive mixture rule, and because of the large numerical value of B_{12}, the method of correlating is very insensitive to the mixture rule.

Probably the major reason for the lack of success in correlation is due to the basic corresponding states criteria being violated. From figure 6.3 benzene and cyclohexane appear to have different temperature functions. Indeed, recent measurements by Eubank et al (1974) indicate that at over 400 K the coefficients of cyclohexane are less negative than those of benzene.

The differing functional form is also highlighted by the two forms of correlation equation illustrated in figure 6.3. The McGlashan-Potter equation fits benzene very well, but is poor for cyclohexane, especially at the higher temperatures.

The modified Pitzer-Curl correlation, however, has a functional shape that fits the cyclohexane results better than the benzene values. The lack of fit of the Pitzer-Curl equation is because it was being used as a predictive equation whereas the McGlashan-Potter equation was being used as a fitting equation. However, the point to be made was the differing functional shape of the two correlations.

Since benzene and cyclohexane are not corresponding fluids, the pseudo-critical property combining rules are probably not valid either. Since the results are not yet precise enough to allow any meaningful test of the various geometric and linear combining rules, little can be said about them.

7-3 Improvements to Experimental Apparatus and Technique

The final section of this chapter will discuss and put forward methods of improving the present apparatus, together with suggestions of modifications ranging from minor points to complete rebuilding of the apparatus, together with construction techniques. Finally, an alternative experimental technique to measure the excess coefficient aimed at reducing the experimental work is discussed.

7-3.1 The Present Apparatus

To enable more precise measurements to be made with the existing apparatus, more detailed information is required about the adsorption behaviour of the components, both as pure components and as a mixture. However, the main piece of information required is the adsorptive area of the apparatus. This may be possible to obtain by making the standard adsorptive tests using pressure measurements of helium at liquid nitrogen temperatures, or by using a well-characterized, highly adsorbing vapour at higher temperatures.

An improvement in the temperature control is still required to ensure that the cylinders do not change temperature relative to each other. As suggested earlier, this could probably be done without requiring more sophisticated controllers by increasing the stirrer power and using double-layer thermostats.

7-3.2 Possible Modifications to the Present Apparatus

Two major possibilities exist to improve the present apparatus: either the reconstruction would be in glass, to improve the adsorption properties, or in stainless steel, as before, paying attention to the now obviously important details of construction and surface finish.

Reconstruction in glass using teflon-glass taps is probably now possible. In this case the only metal in the system would then be the transducer. The advantages would be those of an easier system to build and check, and a

lower adsorptive area, although to achieve the low surface area to volume ratios attainable with metal apparatus, there would be structural problems. Also, the lower adsorptive area improvement may only be minimal, but it would be a much easier material to characterize - its adsorption behaviour and existing adsorption information is more plentiful than for metal surfaces.

Rebuilding the components in stainless steel would require high technical expertise to produce a highly finished surface with the vacuum integrity required of the experiment.

The basic requirements would be:

(i) Radius all corners. The radius should be greater than 10 mm. This makes sure that in the subsequent electropolishing, the electric field will not be badly distributed.

(ii) Make the cylinders in two halves, then join them together circumferentially.

(iii) All welding and brazing of all components should be done in an inert atmosphere. High-temperature oxide films have specific areas up to a thousand times that of low-temperature oxides.

(iv) Before the final joining of any of the components, each should be electropolished as laid out in chapter 5. After the electropolishing and washing, the surfaces should be clean enough for distilled water to wet the surface evenly.

(v) The whole assembly should be baked-out at 300-450^{o}C for several hours at vacuums of better than 0.1 Pa.

7-3.3 Redesign of the Present Apparatus

With minor modifications to the existing type of layout, the present apparatus could be used to measure the pure component second virial coefficients as well.

By using the arrangement illustrated in figure 7-1, with cylinder C1 having about half the volume of cylinders C2 and C3, the pure virial

coefficient may be measured over a wider density range per loading. Cylinders C2 and C3 have to be very nearly the same volume as required for the excess coefficient measurement.

To measure the excess coefficient, component 1 is loaded into cylinders C1 and C2 with valves V2 and V6 closed. The loading pressure is measured using the differential pressure transducer and nitrogen as outlined in chapter 4. Valves V5, V3 and V7 are then closed, valve V6 opened, and the system evacuated. When the evacuation is complete, component 2 is loaded into cylinder C3 and the pressure balanced using the differential transducer. With valve V1 closed, the contents of cylinders C2 and C3 are mixed and the resulting ΔP measured with the transducer.

The pure second virial coefficients may be measured using a method developed by Couldwell et al (1975). Briefly, Couldwell's method consisted of measuring the pressure of a fixed amount of vapour in each of two volumes and then in both of the volumes together. By applying the virial equation of state to each of the three situations, he eliminated the volume term and developed an equation that gave him a B value as a function of his measured pressures. By making a series of measurements with varying number of moles in each, he could make an extrapolation to zero pressure, and hence determine the zero pressure, or the infinite series, second virial coefficient. The slope of this extrapolation is the third virial coefficient. As pointed out by Scott and Dunlap (1962), this procedure is required to obtain the theoretically significant second virial coefficient.

The apparatus illustrated in figure 7-1 has the added advantage over the existing Couldwell apparatus in that seven pressure measurements over a five-fold density range may be made with one loading. The existing, two-volume apparatus gives three pressure measurements over a two-fold density variation per loading.

The measurements could be made by loading the component into cylinder C1 initially, then closing valves V1 and V6, leaving V5 open. The component pressure is then measured using the differential pressure transducer

as a null gauge for each of the cylinders separately, in all the binary combinations, and finally, with all three cylinders together. The Marsh (1975) procedure may also be followed using this arrangement.

7-3.4 An Alternative Experimental Technique

An alternative method of using the existing apparatus was suggested by Dr I.A. McKinnon. His technique consisted of carrying out the measurement as usual. Then, once the pressure change measurement has been made, change the thermostat temperature and measure the new pressure change. After correcting the observed pressure change for the loading pressure difference that would have occurred due to the temperature change, the residual pressure change would be that due to the mixing process at the new temperature.

The analysis of this method has been developed. After a long and detailed analysis, the following expression resulted:

$$\varepsilon(T_2) = \varepsilon(T_2)_{\text{apparent}} - \frac{R(T_2-T_1)}{P} - \frac{1}{2x_2}\left(B_{11}(T_2)-B_{11}(T_1)\right) - \frac{1}{2x_1}\left(B_{22}(T_2)\right.$$

$$\left. - B_{22}(T_1)\right) + \frac{RT_2}{P^2}\left\{\frac{RT_2}{\frac{V}{n_1} - B_{11}(T_2)} - \frac{RT_1}{\frac{V}{n_1} - B_{11}(T_1)}\right\} \qquad (7.1)$$

The first correction term in equation (7.1) arises out of the RT term in the virial equation. The second and third terms are a measure of how unequal the loading pressures would be if the given number of moles of each component were initially confined unmixed at temperature T_2. Lastly, the fourth term is the correction for the change in pressure of the reference cylinder.

Even for small changes in temperature, the magnitude of the $R(T_2-T_1)$ term together with its error plus the large errors of the $(B(T_2)-B(T_1))$ and RT_2/P^2 terms, causes such a large and ill-defined correction as to make the new measurement useless.

CHAPTER 8: CONCLUSIONS

From this study, we may conclude the following:

(i) The ΔP^E method of measuring the excess second virial coefficient is viable, being experimentally straightforward once the equipment was developed and giving highly reproducible results. The pressure transducer employed gave a sensitivity that was more than adequate, although the zero-stability was not good enough using the simple experimental procedure.

(ii) The "open tap" technique successfully overcame the zero-stability problem, for which it was developed. When using this technique, there was no evidence of major or significant errors that could possibly have been caused by pre-mixing of the two vapours, or non-mixing of the vapour left unmixed on the mixing side of the pressure transducer. The "open tap" technique also gave the advantage of removing the cause of any bias in the results if oil were present in the reference cylinder. Also, this technique made the manipulation of the apparatus more straightforward and less critical.

(iii) Under certain conditions, which result from a combination of loading pressure, saturation vapour pressure and temperature, the number of moles loaded into each volume of our equipment was less than 10^{-2} moles, surface adsorption effects become significant, requiring large corrections to be made. Corrections based on a B.E.T. isotherm with adsorption behaviour of benzene and cyclohexane, obtained from the literature, appear to be qualitatively justified. To enable quantitative corrections to be made, more information is required on the adsorption isotherms of both the pure components and their mixtures. Quantitative information would also allow the pin-pointing of the loading pressure as a fraction of the saturation vapour pressure that gives a zero adsorption correction. From the qualitative information our adsorption model gives us, it would appear that

our apparatus has an adsorptive area about twice the geometric area, indicating that a smoother surface, such as that obtained with glass, would give a small increase in the useful temperature range. Attention to the surface finishing of the cylinders and the valve assembly may also achieve this increase. The advantage of a metal assembly is that it makes the large volume to surface area ratios, helpful in reducing the adsorptive effective, easily attainable.

(iv) The ΔH^E on mixing measurement is complementary to the ΔP^E measurement and will, due to its steady-state nature, allow measurements of ε to be made in regions where adsorption would be troublesome to the ΔP^E measurement. These two measurements together promise to enable ε measurements to be made accurately over a wide temperature range.

(v) All traces of oil or liquids capable of absorbing vapour must be removed. The only method that appears to be able to meet this requirement is baking to 300-400^{o}C under high vacuum (0.01 to 0.001 Pa).

(vi) Thermostat temperature control, although not critical in an absolute sense, is highly critical when attempting to maintain constant relative vessel temperatures. The absolute temperature need only be known to 0.1 K, but the vessels must not change relative to each other by more than 10^{-4} or 10^{-3} K. To obtain this level of control, the oil bath control heater must not be allowed to alter its power input by anything but very small amounts. This requires either a double-layer thermostat, with the inner thermostat uncontrolled, or more careful heater placement coupled with intense and highly turbulent mixing of the oil bath. The use of a two-term temperature controller, with a higher resolution sensor, would be necessary after the other modifications had been implemented.

(vii) For the benzene-cyclohexane system, the extrapolation of ε to the zero-pressure limit has a zero slope as, at our operating pressures, the effect of the third virial coefficients is negligible. The analysis

of the results developed in chapter 3 indicates how to estimate the effect of the third virial coefficient on the extrapolation to the zero pressure limit of ε.

(viii) Existing correlations and mixture rules have varying degrees of success in correlating the mixture behaviour. The corresponding states correlations and mixture rules of McGlashan and Potter are poor for ε (a very sensitive test), predicting a near-zero excess coefficient, but within the much larger tolerance of the B_{12} temperature function, provide an acceptable rule. The B_{12} values have much larger errors due to the less well-known B_{11} and B_{22} values that exist. More discerning tests of the mixture rules await more precise pure component coefficients.

Another problem of attempting to correlate the mixture properties using corresponding states is that benzene and cyclohexane are not corresponding fluids. Their temperature functions are not of the same shape and, indeed, at higher temperatures they appear to cross. Hence, the basic assumption of corresponding states (i.e. the same intermolecular potential function) does not appear to hold.

APPENDIX I: THE CORRECTION TO THE APPARENT MOLE FRACTION

If we were to calculate an "apparent" mole fraction x* such that

$$x_1^* = \frac{(n_1/V)}{\frac{n_1+n_2}{V}} \qquad (I.1)$$

where (n_1/V) and (n_2/V) are obtained from equations (3.1 and .2), then the "true" mole fraction would be

$$x_1 = \frac{(n_1 - n_1')}{(n_1-n_1')(n_2-n_2')} \qquad (I.2)$$

where n' is the correction to the number of moles in the vapour phase, so

$$\frac{x_1x_2}{x_1^*x_2^*} = \frac{(n_1-n_1')(n_2-n_2')}{(n_1+n_2-n_1'-n_2')^2} \cdot \frac{(n_1+n_2)^2}{n_1n_2}$$

$$= \frac{(n_1n_2-(n_1n_2'+n_1'n_2))(n_1+n_2)^2}{((n_1+n_2)^2-2(n_1+n_2)(n_1'+n_2'))n_1n_2} \qquad (I.3)$$

neglecting second-order terms.

The numerator of equation (I.3) may be expanded using the binomial theorem since $n_1', n_2' \ll n_1$ or n_2, i.e.

$$\frac{1}{((n_1+n_2)^2-2(n_1+n_2)(n_1'+n_2'))n_1n_2} = \frac{1}{(n_1n_2)(n_1+n_2)^2\{1-\frac{2(n_1'+n_2')}{(n_1+n_2)}\}}$$

$$= \frac{1+\frac{2(n_1'+n_2')}{n_1+n_2}}{(n_1n_2)(n_1+n_2)^2} \qquad (I.4)$$

to first-order terms. Substituting (I.4) into(I.3)gives

$$\frac{x_1x_2}{x_1^*x_2^*} = 1 + \frac{2(n_1'+n_2')}{n_1+n_2} - \frac{n_1'}{n_1} - \frac{n_2'}{n_2} \qquad (I.4)$$

after neglecting second and higher order terms.

For our experiments, $n_1 \simeq n_2 \simeq 0.01$ mol and for $n_1' \simeq 2n_2' \simeq 0.001$ mol

$$\frac{x_1 x_2}{x_1^* x_2^*} = 1.05$$

i.e. a gross change in the number of moles in the vapour phase only produces a five percent change in the apparent mole fraction product. The change in the number of moles in the vapour phase that we could expect in our experiments would be about 2×10^{-4} moles. This would cause our differential pressure transducer to overload. Normally the change in the number of moles in the vapour phase would be about 10^{-6} or 10^{-7} moles, so we will not distinguish between the apparent and true mole fractions in our analysis.

APPENDIX II: AN ALTERNATIVE ANALYSIS OF THE DATA TREATMENT

This analysis was developed by Knobler (1959 and Feb. 1967). It differs from the analysis presented in section 3-1 by using the volumetric virial coefficients directly.

Starting as in section 3-1, only using

$d_i = n_i/V$, i.e. d_i is the molar density (in moles$(m^3)^{-1}$) of component i

and the volumetric virial equation of state, then

$$P = d_1RT(1 + B_{11}d_1 + C_{111}d_1^2 \ldots) \qquad \text{(II.1)}$$

and

$$P = d_2RT(1 + B_{22}d_2 + C_{222}d_2^2 + \ldots) \qquad \text{(II.2)}$$

Upon mixing we may write

$$P_m = d_mRT(1 + B_m d_m + C_m d_m^2 + \ldots) \qquad \text{(II.3)}$$

Now $d_m = \frac{1}{2}(d_1 + d_2)$ (II.4)

and defining $\Delta P = P_m - P$ as before, then when equations (II.1 and .2) are subtracted from (II.3) and the substitutions made

$$\frac{2\Delta P}{RT} = \frac{1}{2}(d_1+d_2)^2B_m - B_{11}d_1^2 - B_{22}d_2^2 + \frac{1}{4}(d_1+d_2)^2C_m - C_{111}d_1^3 - C_{222}d_2^3 + \ldots \qquad \text{(II.5)}$$

Using the definitions for ε, $\mathcal{J}_1$ and $\mathcal{J}_2$ set out in Chapter 1 along with the expressions for C_m and B_m, we obtain

$$\frac{2\Delta P}{RT} = d_1d_2\varepsilon + \tfrac{1}{2}(d_1-d_2)(B_{22}d_2-B_{11}d_1) + d_1^2d_2(\tfrac{3}{4}\mathcal{J}_1 + \tfrac{1}{2}C_{111} + \tfrac{1}{4}C_{222}) + d_1d_2^2(\tfrac{3}{4}\mathcal{J}_2 + \tfrac{1}{2}C_{222} + \tfrac{1}{4}C_{111}) - \tfrac{3}{4}(d_1^3C_{111} + d_2^3C_{222}) + \ldots \qquad \text{(II.6)}$$

Dividing equations (II.1 and .2) by RT and inverting, gives

$$d_i = (\frac{P}{RT}) - B(\frac{P}{RT})^2 + (2B^2 - C)(\frac{P}{RT})^3 + \ldots \qquad \text{(II.7)}$$

Substituting using (II.7) in (II.6) gives, finally,

$$\{1-(B_{11}+B_{22})(\frac{P}{RT})\}\varepsilon = \frac{2RT\,P}{P^2} - \{\frac{1}{2}(B_{22}-B_{11})^2 + \frac{3}{4}(\mathcal{F}_1+\mathcal{F}_2)\}\ (\frac{P}{RT})$$

$$+ \text{terms in ascending powers of } (P/RT) \qquad \text{(II.8)}$$

Since the $(B_{11}+B_{22})(P/RT)$ term is small in relation to 1, the binomial theorem may be used to expand

$$\{1-(B_{11}+B_{22})\ \frac{P}{RT}\}^{-1} = 1+(B_{11}+B_{22})\frac{P}{RT} - ((B_{11}+B_{22})\frac{P}{RT})^2 + \ldots \qquad \text{(II.9)}$$

Substituting this into equation (II.8) gives the final result

$$\varepsilon = \frac{2RT\Delta P}{P^2} - \{\frac{1}{2}(B_{22}-B_{11})^2 - \varepsilon(B_{11}+B_{22}) + \frac{3}{4}(\mathcal{F}_1+\mathcal{F}_2)\}(\frac{P}{RT})$$

$$+ \text{further terms in } C,\ B^2,\ \varepsilon, \text{ and } \text{ as an ascending series in } (P/RT)^n \qquad \text{(II.10)}$$

APPENDIX III: THE EFFECT OF UNEQUAL MIXING VOLUMES

Using the same notation as in Chapter 3-2 and putting $V_1 = V = V_2 - \delta V$ where δV is a small difference in volume, then equation (3-10) becomes

$$\delta x_1 + x_1 = \frac{(n_1 + n)/V}{\frac{n_1+\delta n}{V} + \frac{n_2+\delta n}{V+\delta V}} \qquad \text{(III.1)}$$

Multiplying out, collecting terms, ignoring second-order terms, and subtracting

$\frac{n_1}{V} = x_1 \frac{n_1}{V} + x_1 \frac{n_2}{V+\delta V}$ from each side of the equation, then gives

$$\delta x_1 \left(\frac{n_1}{V} + \frac{n_2}{V+\delta V}\right) = \frac{\delta n}{V} - \frac{\delta n}{V} x_1 \left(1 + \frac{V}{V+\delta V}\right) + \frac{n_2}{V} x_1 \left(1 - \frac{V}{V+\delta V}\right) \qquad \text{(III.2)}$$

$$\text{i.e.} \quad \frac{\delta x_1}{x_1} = \frac{\delta n/V}{x_1\left(\frac{n_1}{V} + \frac{n_2}{V+\delta V}\right)} + \frac{\left(\frac{\delta n}{V}\right)\left(1 + \frac{V}{V+\delta V}\right)}{\left(\frac{n_1}{V} + \frac{n_2}{V+\delta V}\right)} + \frac{\left(\frac{n_2}{V}\right)\left(1 - \frac{V}{V+\delta V}\right)}{\left(\frac{n_1}{V} + \frac{n_2}{V+\delta V}\right)} \qquad \text{(III.3)}$$

since the maximum error is required.

In our apparatus $\delta V/V = 0.002$, i.e. $V+\delta V = 1.002\ V$.

Putting this value into equation (III.3), gives

$$\frac{\delta x_1}{x_1} = \frac{\delta n/V}{x_1\left(\frac{n_1}{V} + \frac{n_2}{1.002V}\right)} + \frac{2.002\ \frac{\delta n}{V}}{\frac{n_1}{V} + \frac{n_2}{1.002V}} + \frac{\frac{n_2}{V}\left(1 - \frac{1}{1.002}\right)}{\frac{n_1}{V} + \frac{n_2}{1.002V}}$$

which approximates equation (3.12), i.e.

$\frac{\delta x}{x} = \frac{\delta n}{n_1} + \frac{2\delta n}{(n_1+n_2)}$ to better than one part per thousand.

APPENDIX IV MEASUREMENTS MADE WITH OIL PRESENT

Run No.	Temperature K to ±0.01 K	Loading Pressure Pa to ±10 Pa	Pressure Change Pa	ε $\frac{m^3\ mol^{-1}}{10^{-6}}$	Reference Component
15	298.16	10,000	14.5±2	720±100	Cyclohexane
16	"	10,000	12.5±2	620±100	Benzene
17	"	10,100	16.6±2	820±100	Cyclohexane
6	323.16	22,200	1.4±0.1	15±1	Benzene
7	"	22,600	1.8±0.1	19±1	"
8	"	22,100	1.7±0.2	19±2	"
9	"	23,000	3.4±0.1	35±1	Cyclohexane
10	"	22,400	3.5±0.1	37±1	"
11	"	22,800	4.2±0.1	43±1	"
12	"	22,400	1.8±0.3	19±3	Benzene
18	"	20,500	1.72±0.07	22±0.3	"
20	"	22,900	4.80±0.07	49±1	Cyclohexane
21	"	12,400	-0.73±0.07	-25±2	Benzene
22	"	12,400	0.17±0.07	6±2	Cyclohexane
13	373.16	40,900	6.0±0.5	22±2	Benzene
14	"	39,100	5.6±1.0	23±4	Cyclohexane

APPENDIX V THERMOSTAT BATH PROPORTIONAL TEMPERATURE CONTROLLER

after M.L. Martin, Adelaide University, South Australia

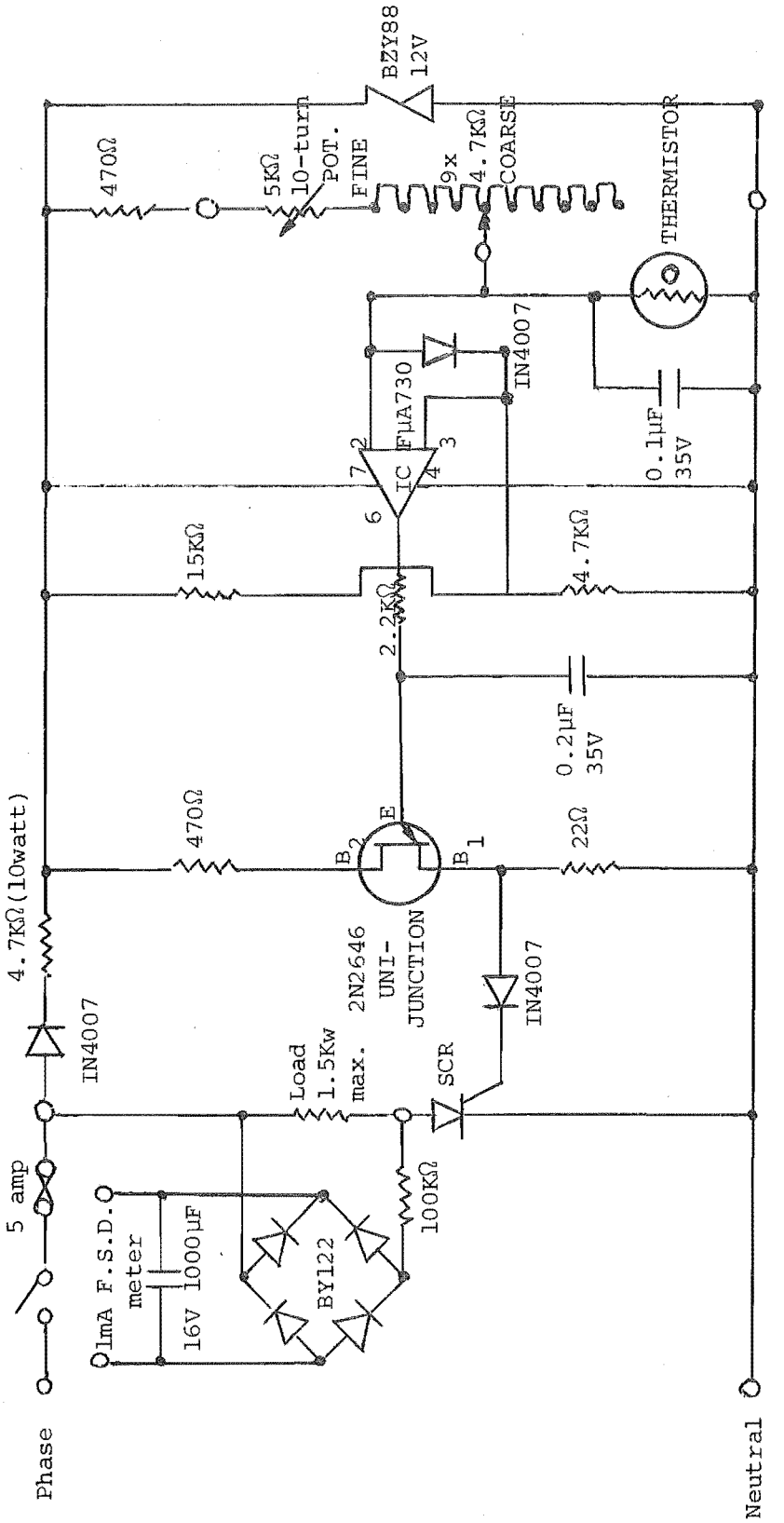

APPENDIX VI: REFERENCES

Babernics L., Tetenyi P., Kertesz L., Zeitschrift fur Physikalische Chemie Neue Folge Bol 89 p 237-48 (1974)

Barker J.A. and Linton M., J. Chem. Phys. 38 p 1953 (1963)

Battino R., Banzhof M., Bogan M., and Wilhelm E., Analyt. Chem. 43, 6, p 806 (May 1971)

Bell T.N., Cussler E.L., Harris K.R., Pepela C.N., and Dunlop P.J., J. Phys. Chem. 72, 3, p 4693 (Dec. 1968).

Bottomley G.A. and Coopes I.H., Nature 193 p 268 (1962)

Brewer J. and Vaughan G.W., J. Chem. Phys. 50, 7, p 2960 (April 1969)

Chan S.H., Project Report for B.E.(Chem.), University of Canterbury, N.Z. (1976)

Chueh P.L. and Prausnitz J.M., A.I.Ch.E.J. 13, 5, p 896 (Sept 1967)

Couldwell C.M., Ph.D. Thesis, University of Canterbury, N.Z. (1975)

Couldwell C.M., O'Neill S.P., Pandya M.V. and Williamson A.G., to be published (1976)

Cox J.D. and Laurenson J.J., Chemical Thermodynamics, Vol. 1, London, John Wright and Sons (1973)

Cox J.D. and Stubley D., Appendix to Partington et al, Trans. Far. Soc. 56 p 484 (1960)

Cruickshank A.J.B., Windsor M.L. and Young C.L., Proc. Roy. Soc. A295 p 259 (1966)

Dymond J.H. and Smith E.B., The Virial Coefficients of Gases, Clarendon Press, Oxford (1969)

Edwards A.E. and Roseveare W.E., J. Am. Chem. Soc. 64, p 2816 (Dec. 1942)

Eubank P.T., Anthony G.G. and Kerns W.J., A.I.Ch.E. Symp. Series, 70, 140, p 14 (1974)

Gorski R.A. and Miller J.G., J. Am. Chem. Soc., 75, p 550 (Feb. 1953)

Guggenheim E., Wormald C.J., J. Chem. Phys. 42, p 3775 (1965)

Hall K.R. and Eubank P.T., A.I.Ch.E.J., 20, 4, p 815 (July 1974)

Hill T.L., Introduction to Statistical Thermodynamics, Addison-Wesley, Reading (1962)

Hirschfelder J.O., Curtiss C.F. and Bird R.B., Molecular Theory of Gases and Liquids, John Wiley, New York (1954)

Knobler C.M., Beenakker J.J.M. and Knapp H.F.P., Physica 25 p 909 (1959)

" Rev. Sci. Inst. 38, 2, p 184 (Feb 1967)

" Dantzler E.M. and Windsor M.L., J. Phys. Chem. 72,2, p 676 (Feb 1968)

" and Dantzler E.M., ibid, 73, 5, p 1335 (May 1969)

" and Dantzler E.M., ibid, 73, 5, p 1602 (May 1969)

" and Dantzler-Siebert E.M., ibid, 75, 25, p 3863

" and Pasco N. Personal communication (1975)

" To be published (1976)

Marsh K.N. and Ewing M.B., Quatrieme Conf. Inter. de Thermo. Chimque, Montpellier IX Section VIII/13, p 128 (1975)

Martin M.L., University of Adelaide, Personal communication (1968)

Mason E.A. and Spurling T.H., The Virial Equation of State, Pergamon Press, Oxford (1969)

Mayhew C.J., Dept of Chem. Eng., University of Canterbury, N.Z. Personal communication (1976)

McElroy P.J., Ph.D. Thesis, University of Otago, N.Z. (1968)

McGlashan M.L. and Potter D.J.B., Proc. Roy. Soc. A267, p 214 (1962)

Pandya M.V. and Williamson A.G., Austral. J. Chem. 24 p 465 (1971)

Prausnitz J.M., Molecular Thermodynamics of Fluid-phase Equilibria, Prentice-Hall, Englewood Cliffs, N.J. (1969)

Scott R.L. and Dunlap R.D., J. Phys. Chem. 66 p 639 (1962)

Tsonopoulos C., A.I.Ch.E.J., 20, 2, p 263 (Mar. 1974)

Waelbroeck F.G., J. Chem. Phys. 23, p 749 (1955)

Weast R.C. (Ed.), Handbook of Chemistry and Physics, 51st Edn, The Chemical Rubber Co., Cleveland (1970)

Wormald C.J., Francis P.G., McGlashan M.L., J. Chem. Thermodynamics, 1, p 441 (1969a)

Wormald C.J., Proc. 1st Internat. Conf. of Calorimetry and Thermodynamics, Warsaw, p 601 (1969b)

FIGURE 3-1

OUR MIXTURE EXPERIMENT

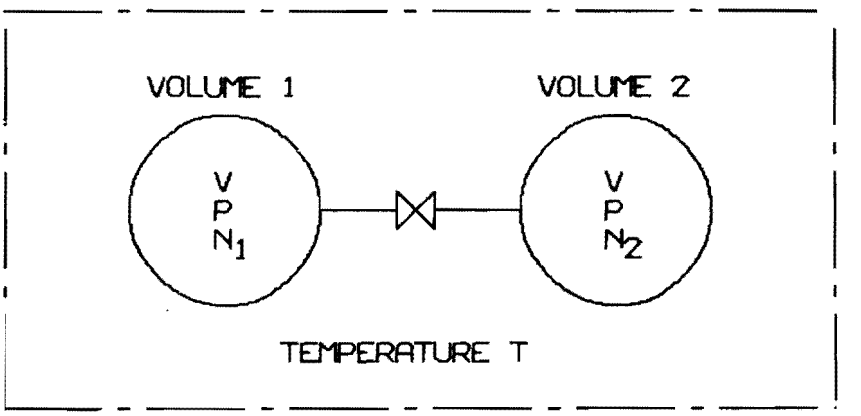

FIGURE 3-2

THE EXPERIMENTAL LAYOUT

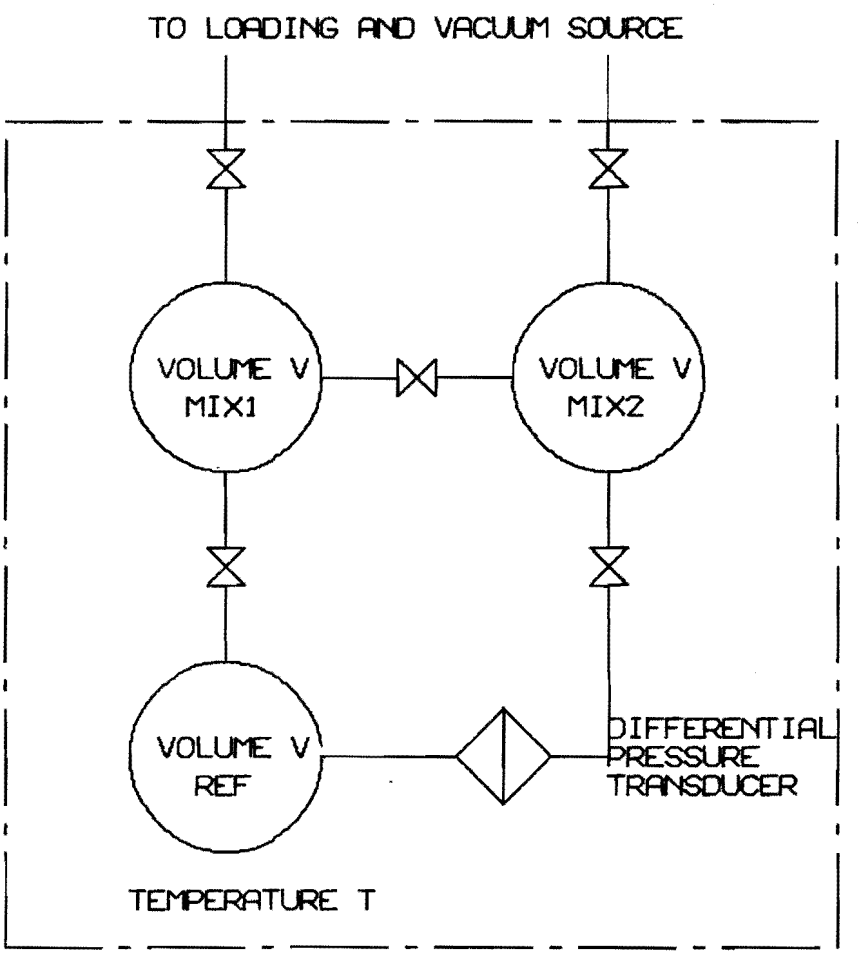

FIGURE 3-3

THE EFFECT OF OIL-INDUCED VAPOUR ABSORPTION

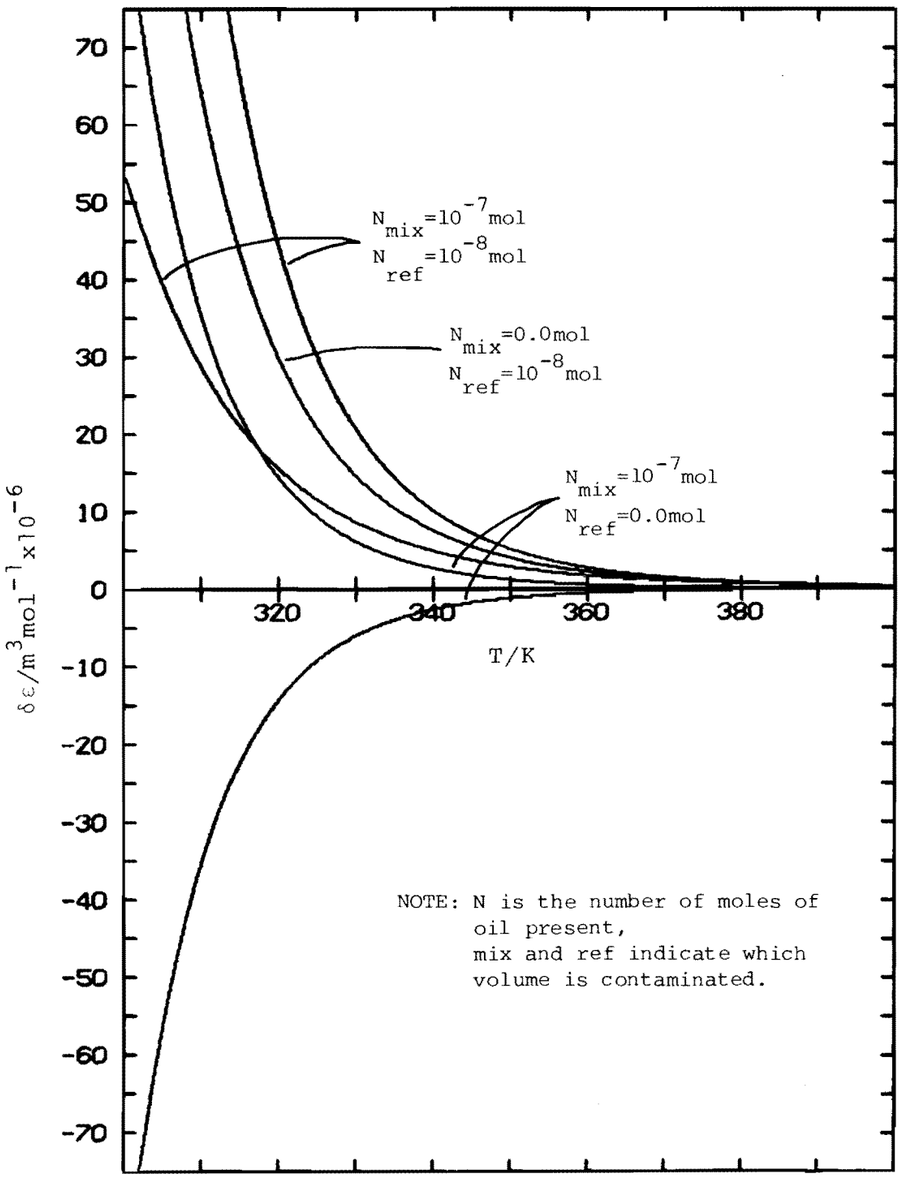

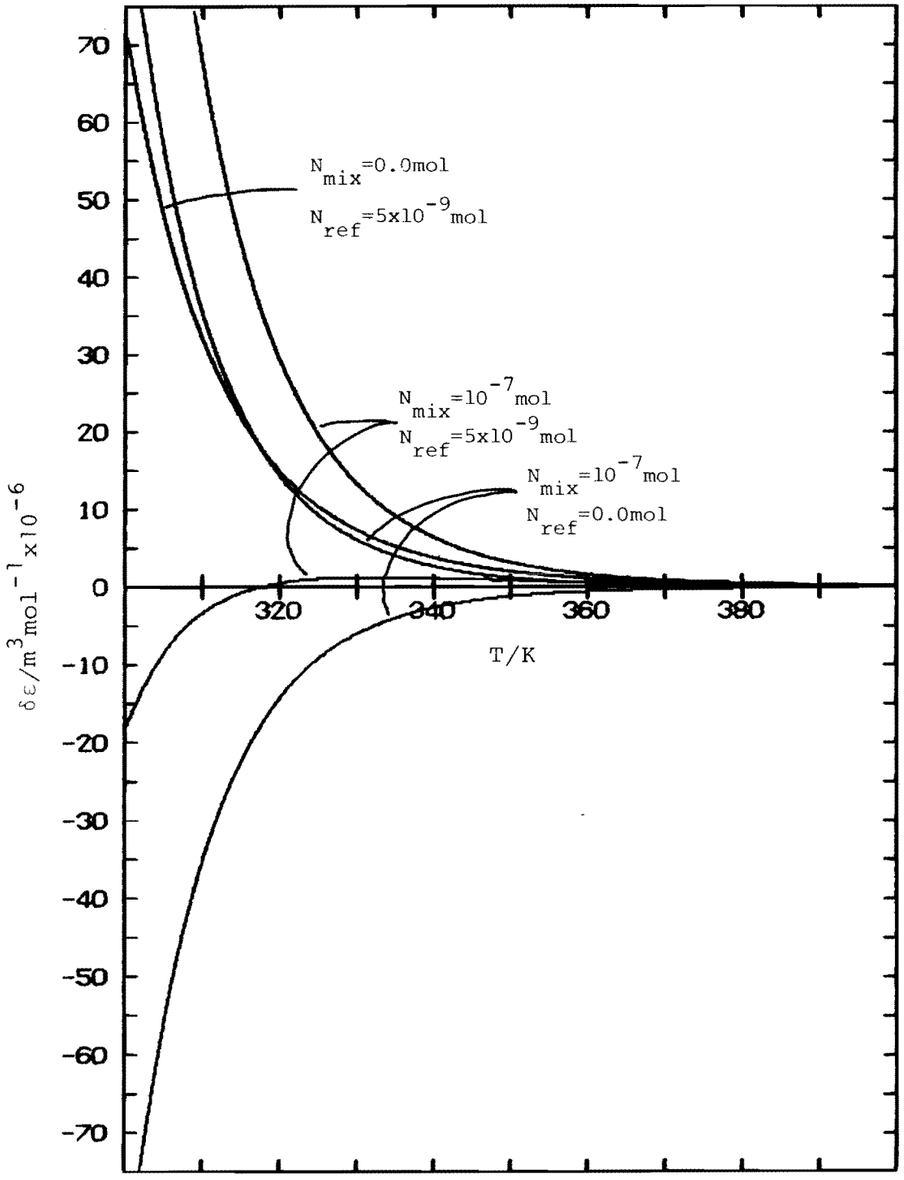

FIGURE 3-4

THE EFFECT OF VAPOUR SURFACE ADSORPTION

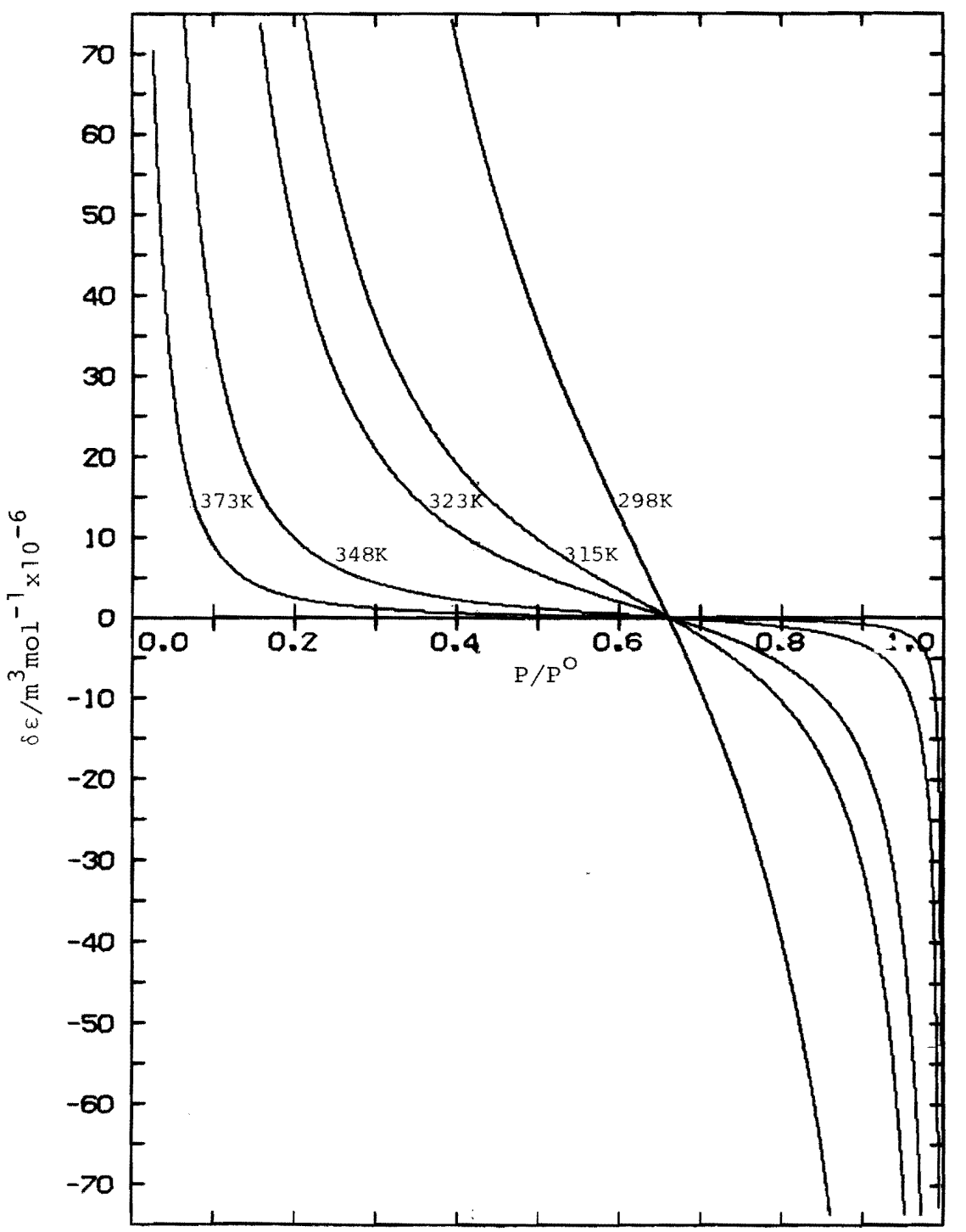

FIGURE 3-5

ADSORPTION ISOTHERM VARIATION WITH ISOTHERM PARAMETER

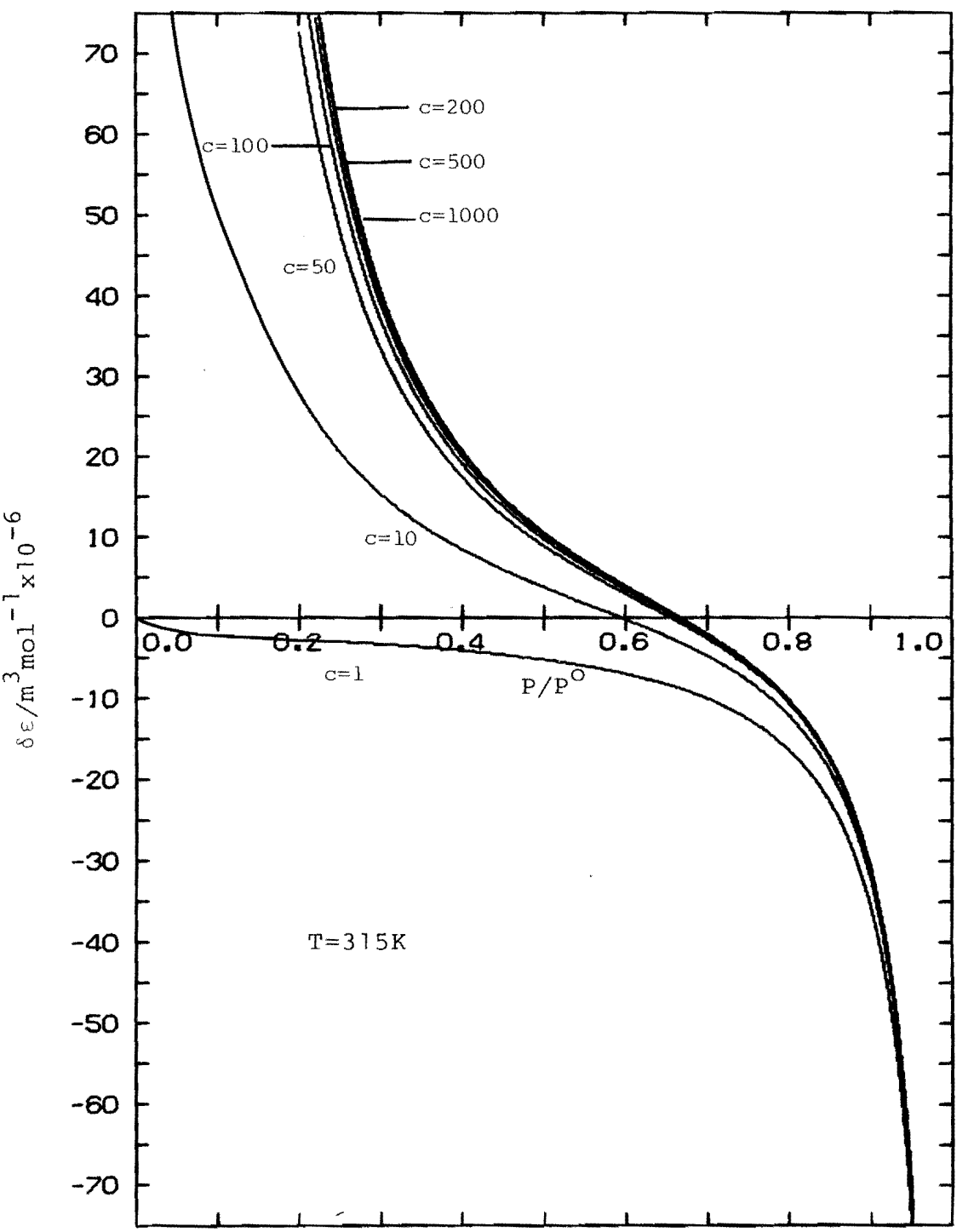

FIGURE 3-6

THE VAPOUR SURFACE ADSORPTION VARIATION WITH AREA

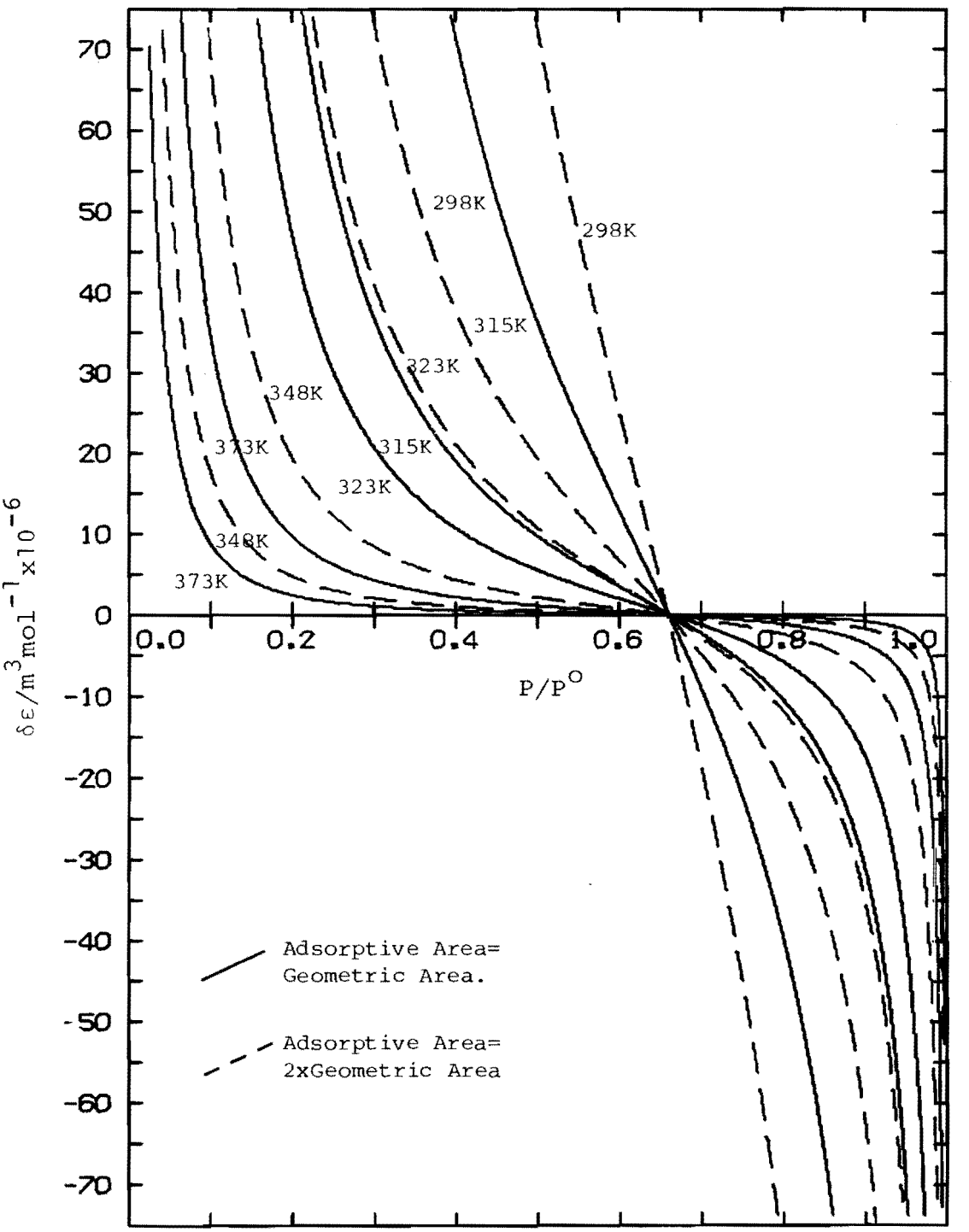

FIGURE 3-7
THE ENERGY TRANSFER ABOUT ONE CYLINDER

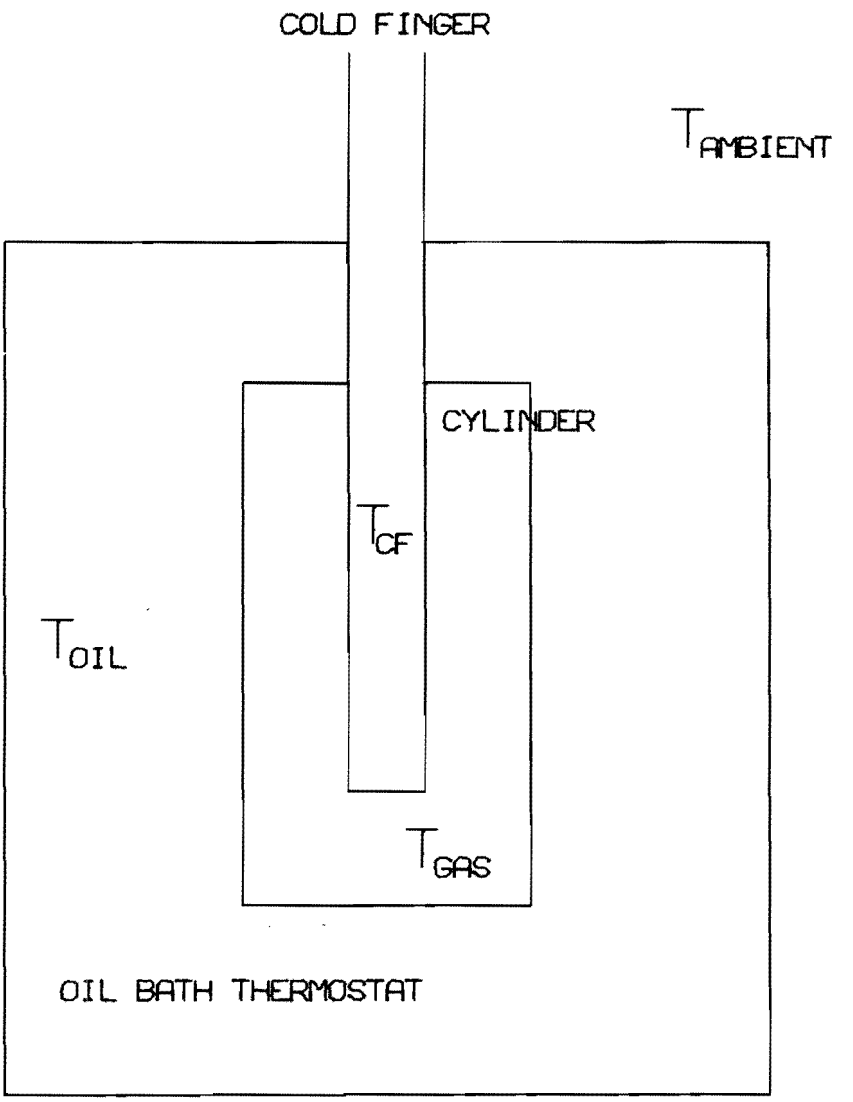

FIGURE 4-1 APPARATUS LINE DIAGRAM

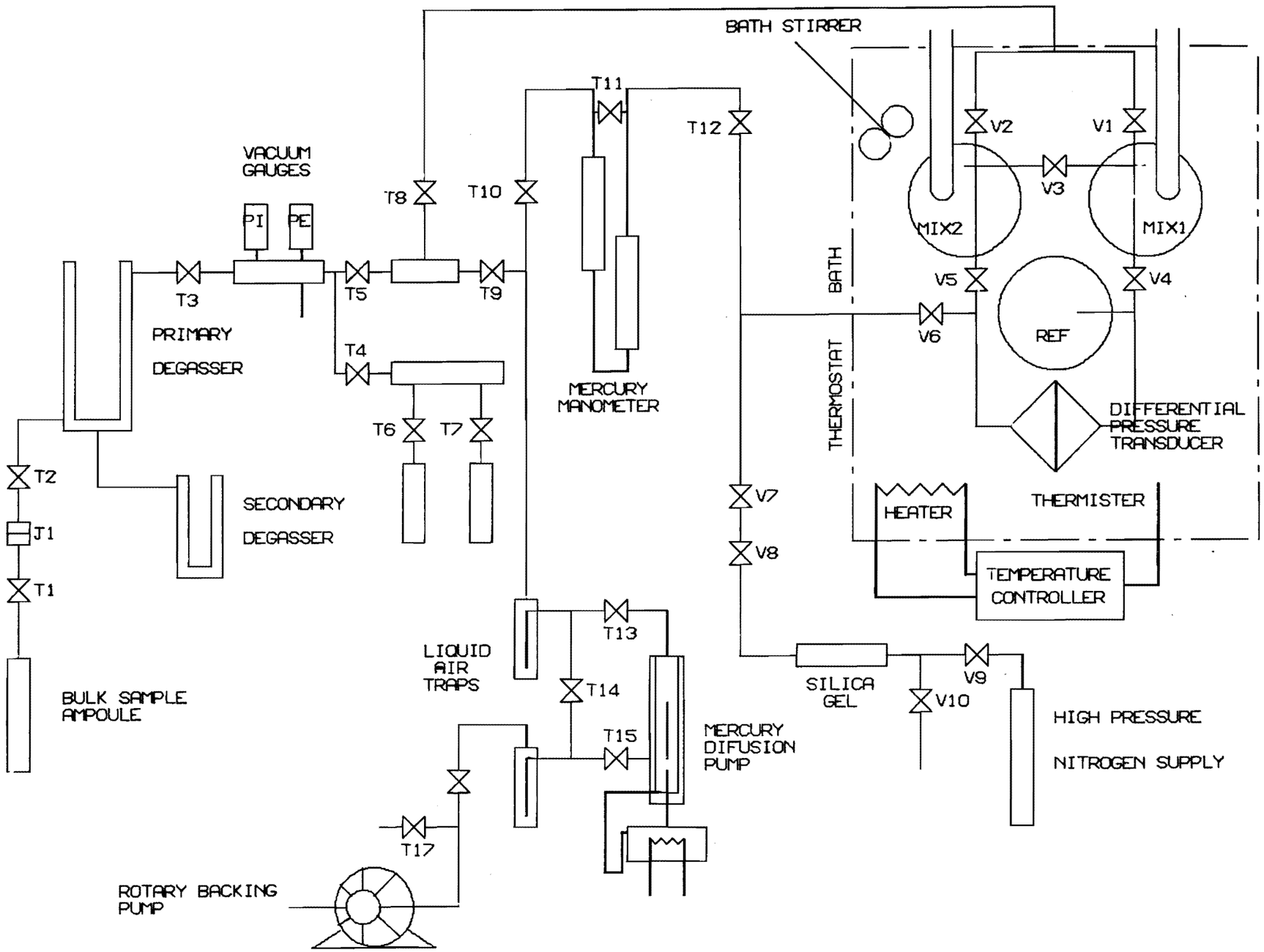

FIGURE 5-1

SAMPLE DEGASSER

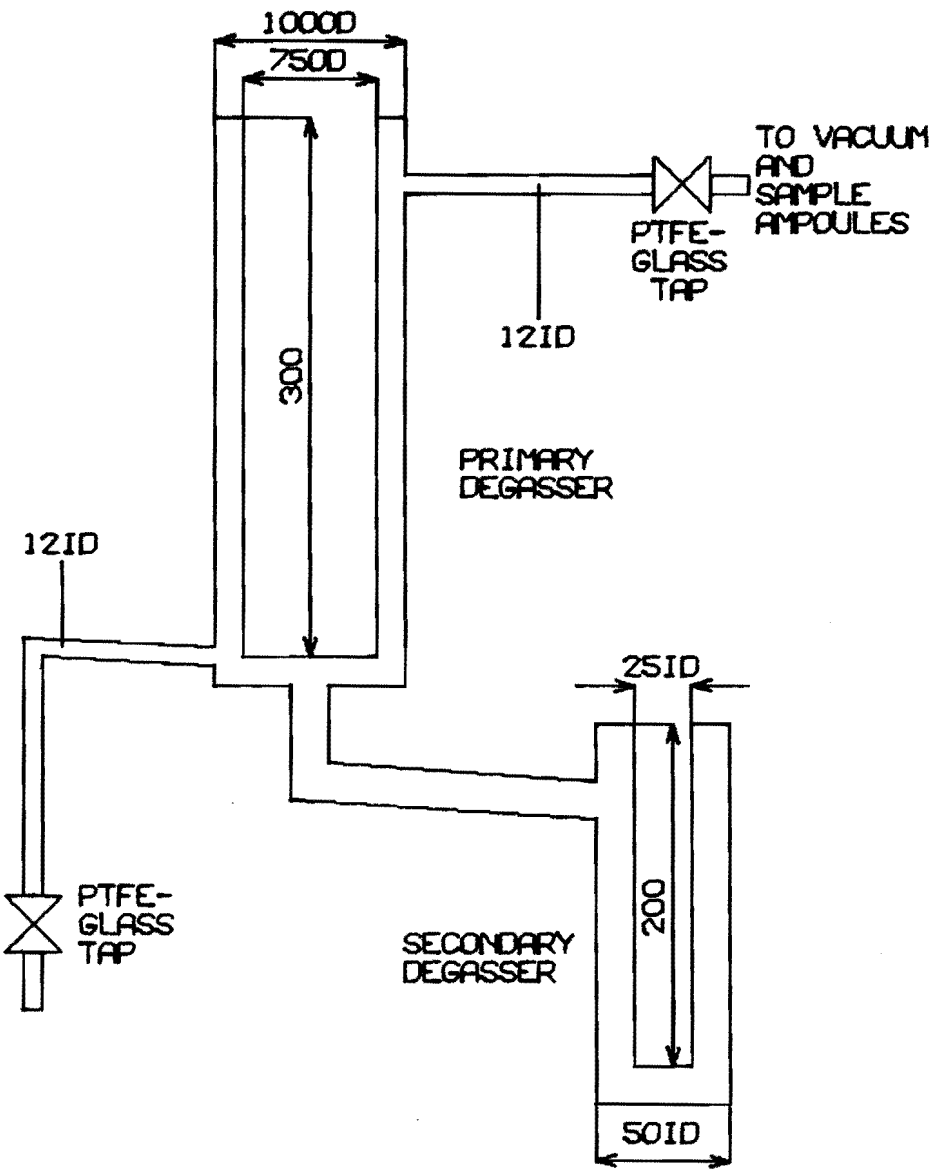

PYREX GLASS CONSTRUCTION

ALL DIMENSIONS IM MM
DO NOT SCALE

FIGURE 5-2
BARATRON DIFFERENTIAL PRESSURE TRANSDUCER

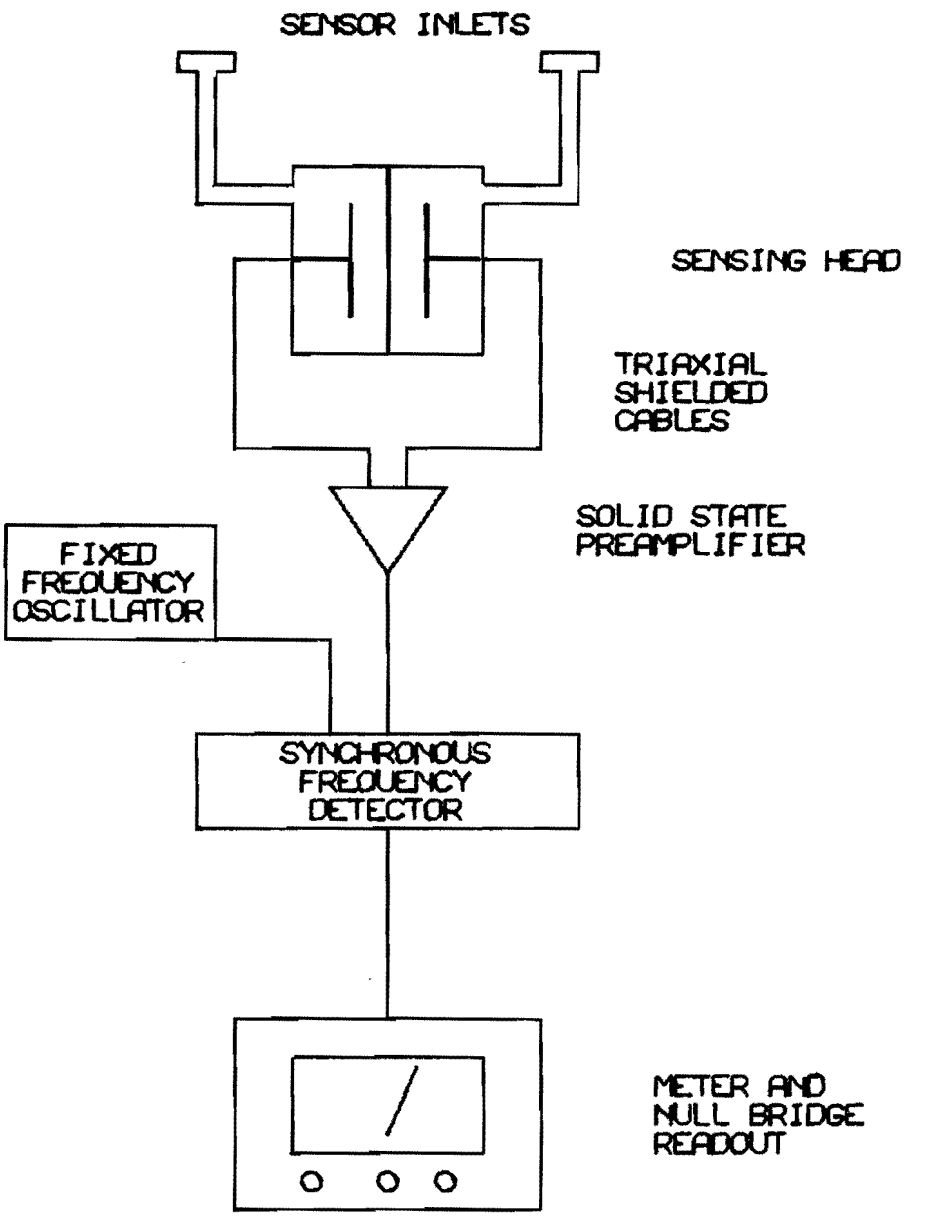

FIGURE 5-3
CONSTRUCTION OF CYLINDERS AND COLD FINGERS

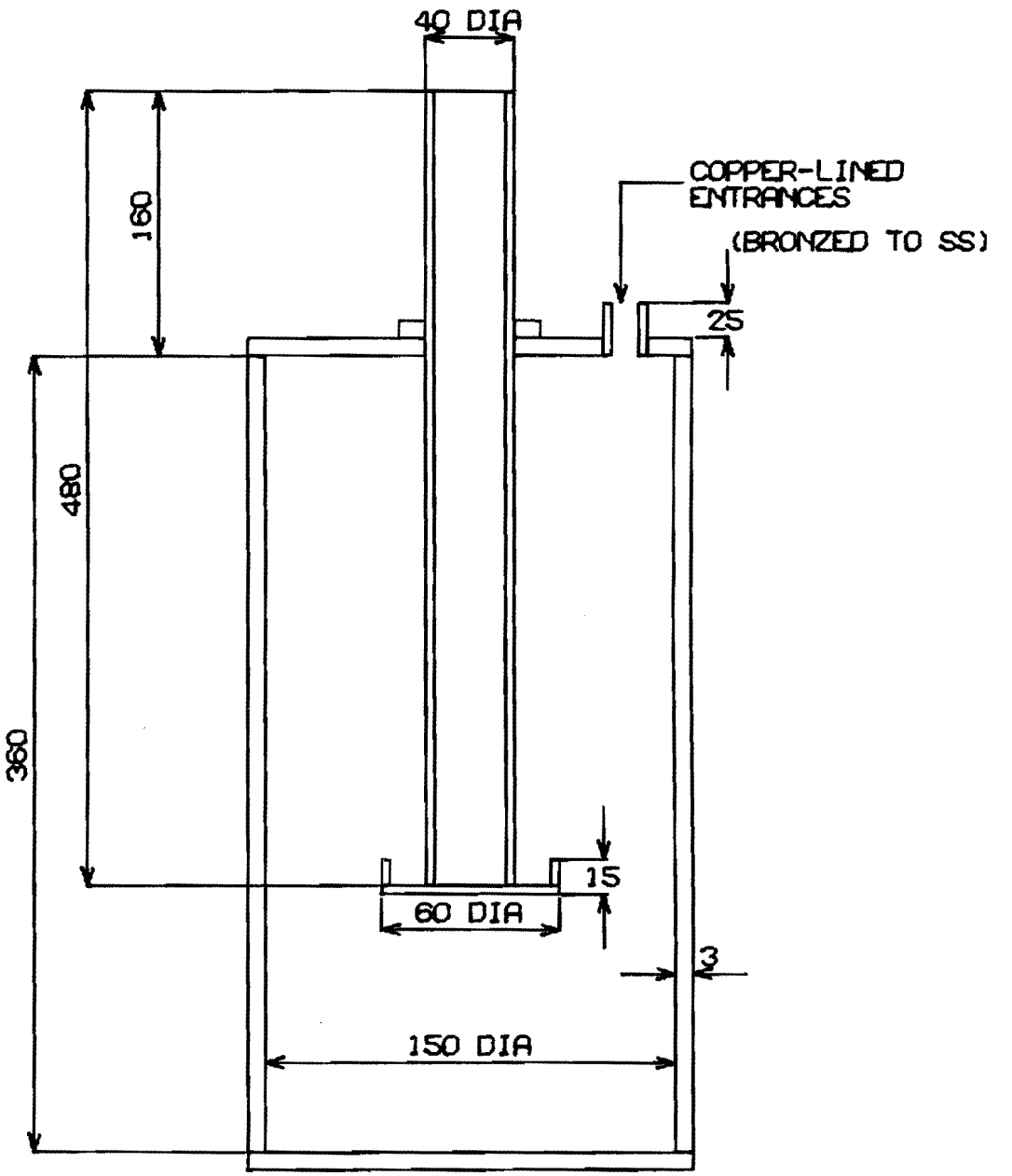

316 STAINLESS STEEL CONSTRUCTION
ALL JOINTS ARGON ARC WELDED

ALL DIMENSIONS IN MM
DO NOT SCALE

FIGURE 5-4

GENERAL LAYOUT OF VALVES AND CYLINDERS

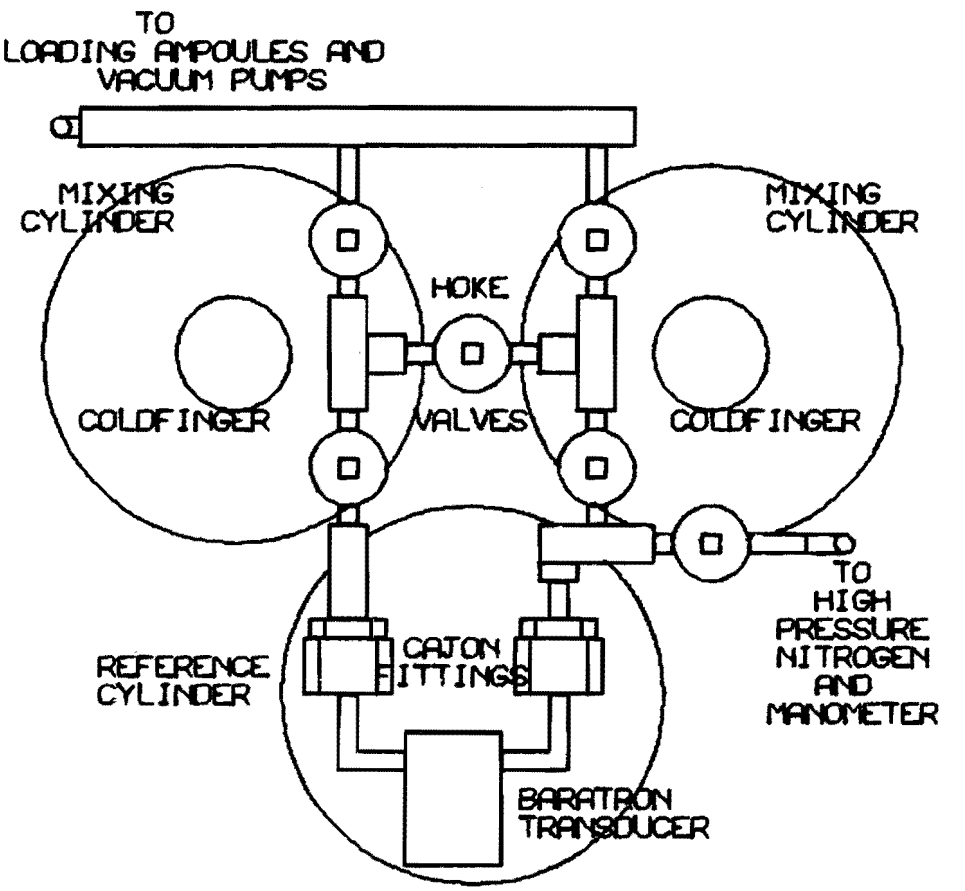

MATERIALS OF CONSTRUCTION
CYLINDERS-316SS
CAJON FITTINGS-316SS
BARATRON TRANSDUCER-316SS AND INCONEL
HOKE VALVES-MONEL
VALVE CONNECTORS-BRASS

FIGURE 6-1

THE EXCESS SECOND VIRIAL COEFFICIENTS OF BENZENE-CYCLOHEXANE

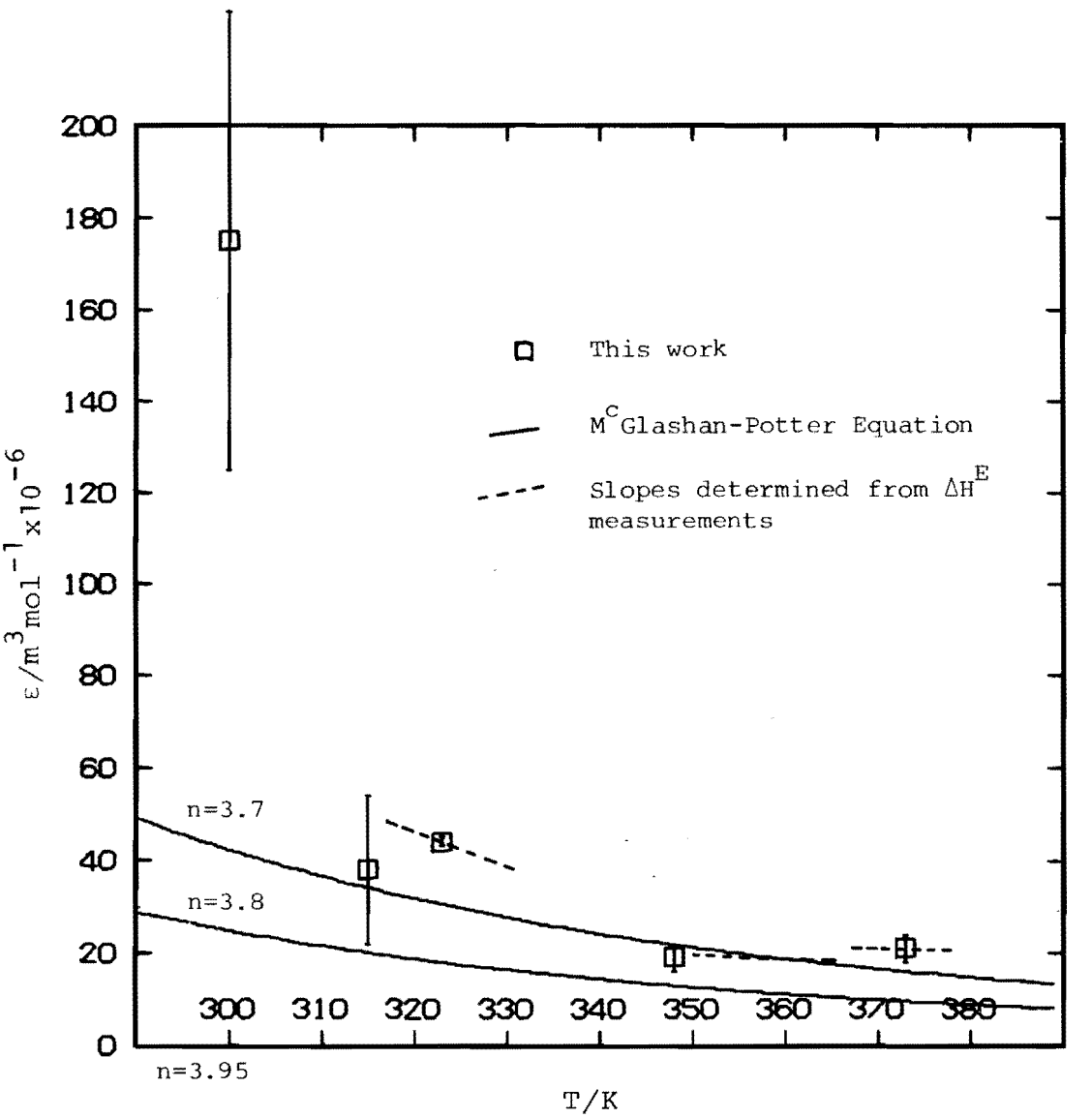

FIGURE 6-2

LITERATURE VALUES FOR THE EXCESS SECOND VIRIAL COEFFICIENTS OF BENZENE-CYCLOHEXANE

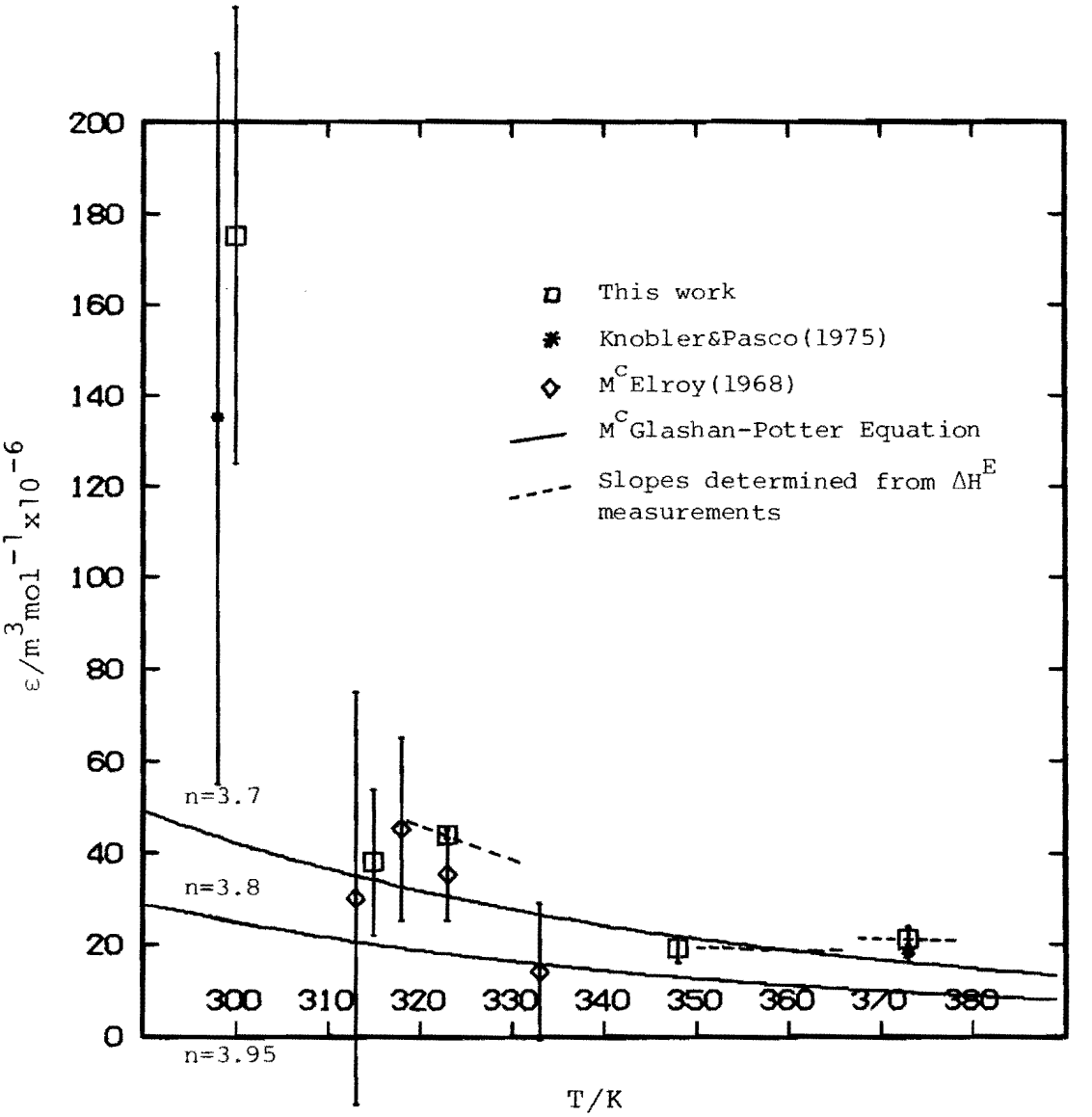

FIGURE 6-3

PURE SECOND VIRIAL COEFFICIENTS OF BENZENE AND CYCLOHEXANE (AFTER DYMOND AND SMITH-1968)

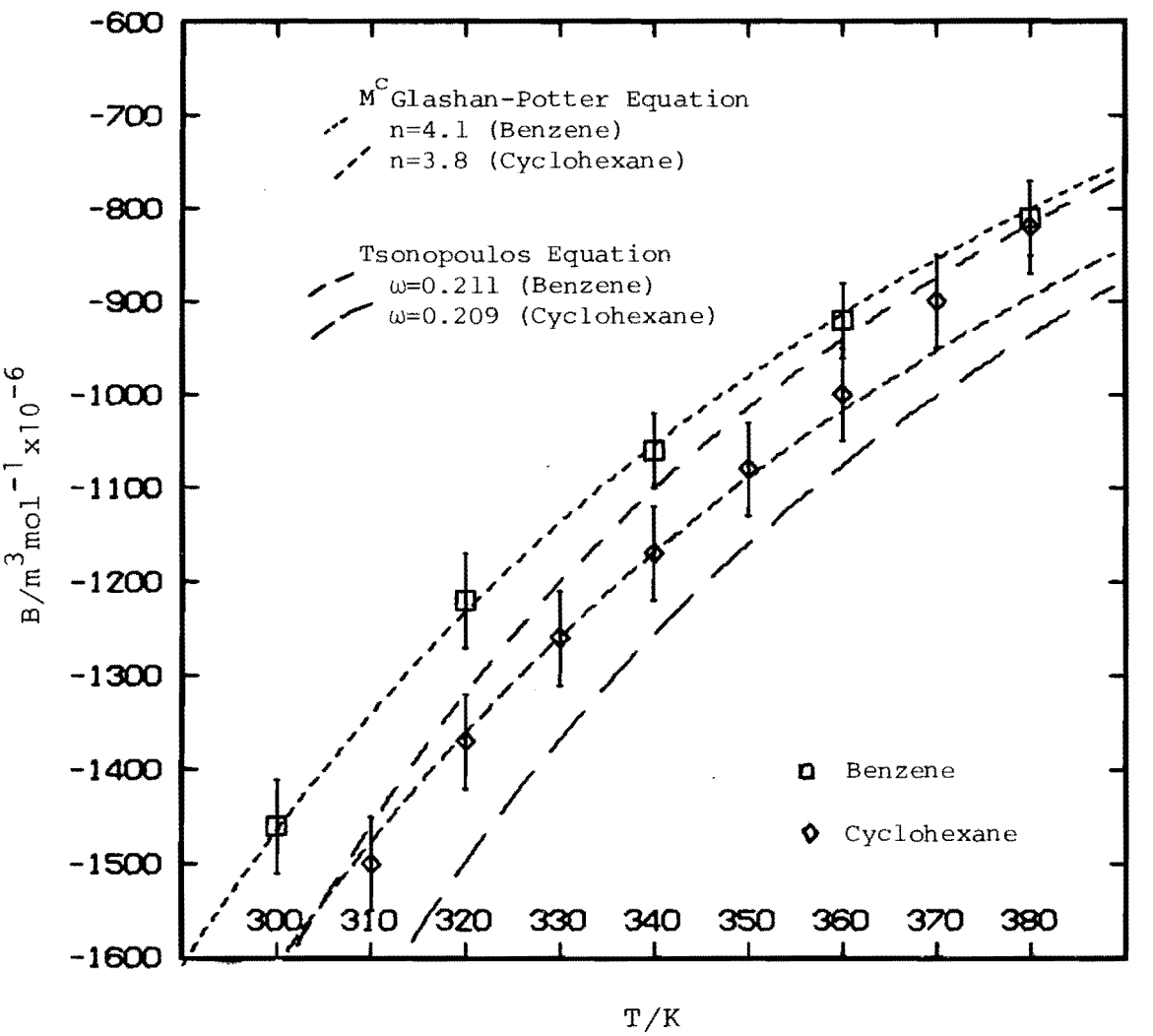

FIGURE 6-4

LITERATURE VALUES FOR THE INTERACTION SECOND VIRIAL COEFFICIENTS OF BENZENE-CYCLOHEXANE

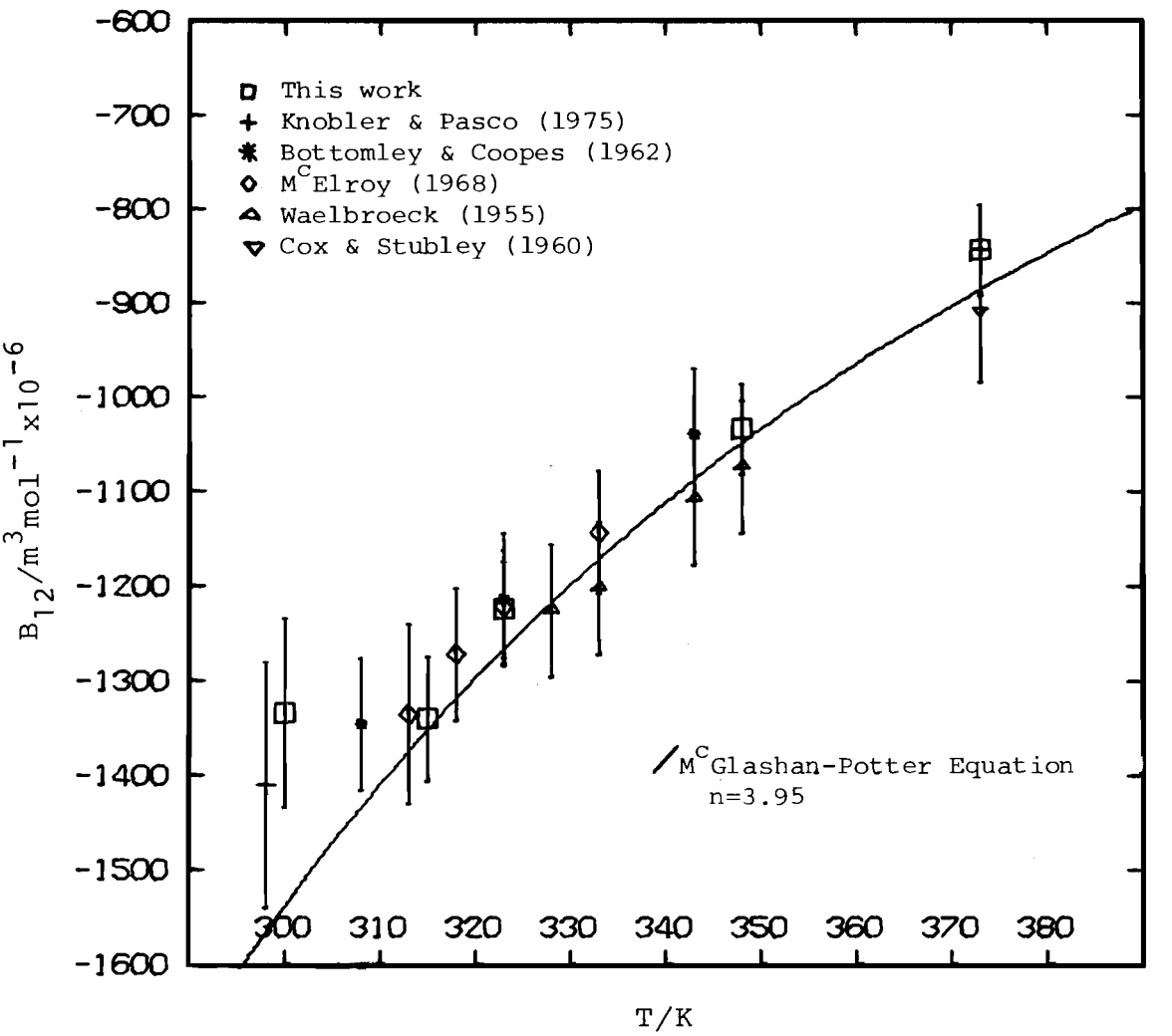

FIGURE 7-1
AN APPARATUS TO MEASURE PURE AND EXCESS SECOND VIRIAL COEFFICIENTS